JPG | Journal of Petroleum Geology

NEW GEOCHEMICAL INSIGHTS INTO CENOZOIC SOURCE ROCKS IN AZERBAIJAN: IMPLICATIONS FOR PETROLEUM SYSTEMS IN THE SOUTH CASPIAN REGION

V. Aghayeva[1], R. F. Sachsenhofer[1*], C.G.C. van Baak[2], A. Bechtel[1], T. M. Hoyle[2], D. Selby[3,4], N. Shiyanova[5] and S. J. Vincent[2]

The Maikop Group and the Diatom Formation constitute the two main source rocks in the South Caspian Basin and onshore Azerbaijan where large-scale oil production began more than 150 years ago. However, the stratigraphic distribution of the source rocks and the vertical variation of source-rock parameters are still poorly understood. The aim of the present paper is therefore to investigate in high resolution the source-rock distribution in the Perekishkyul and Islamdag outcrop sections, located 25 km NW of Baku, which provide nearly complete middle Eocene and lower Oligocene to upper Miocene successions. Bulk geochemical parameters of 376 samples together with maceral, biomarker and isotope data were analysed. In addition, new Re/Os data provide independent age dating for the base of the Upper Maikop Formation (30.0 ± 1.0 Ma) and the paper shale within the Diatom Formation (7.2 ± 2.6 Ma). The presence of steradienes in high concentrations demonstrates the thermal immaturity of the studied successions, limiting the application of some biomarker ratios.

Intervals with high TOC contents and containing kerogen Type II occur near the top of the middle Eocene succession. However, because of the low net thickness, these sediments are not considered to constitute significant hydrocarbon (HC) source rocks. The Maikop Group in the Islamdag section is 364 m thick and represents lower Oligocene (upper Solenovian) to middle Miocene (Kozakhurian) levels. Samples are characterized by moderately high TOC contents (~1.8 wt.%) but low hydrogen index (HI) values (average ~120 mgHC/gTOC) despite a dominance of aquatic organic matter (diatoms, methanotrophic archaea and sulphate-reducing bacteria). Rhenium-osmium chronology suggests low sedimentation rates

[1]Chair in Petroleum Geology, Montanuniversitaet Leoben, 8700 Leoben, Austria.
[2]CASP, West Building, Madingley Rise, Madingley Road, Cambridge, CB3 0UD, United Kingdom
[3]Department of Earth Sciences, University of Durham, Durham DH1 3LE, United Kingdom
[4]State Key Laboratory of Geological Processes and Mineral Resources, School of Earth Resources, China University of Geosciences, Wuhan, China 430074
[5]BP Azerbaijan, Baku, Azerbaijan.
* corresponding author, email:
    reinhard.sachsenhofer@unileoben.ac.at

(~25 m/Ma), which may have had a negative impact on organic matter preservation. Terrigenous organic matter occurs in variable but typically low amounts. If mature, the Maikop Group sediments at Islamdag could generate about 2.5 tHC/m².

The Diatom Formation includes a 60 m thick paper shale interval with high TOC contents (average 4.35 wt.%) of kerogen Type II-I (HI up to 770 mgHC/gTOC). The source potential is higher (~3 tHC/m²) than that of the Maikop Group. The organic matter is dominated by algal material including diatoms. High TOC/S ratios suggest deposition under reduced salinity conditions. Strictly anoxic conditions are indicated by the presence of biomarkers for archaea involved in methane cycling.

For oil-source correlations and a better understanding of the petroleum system, it will be necessary to distinguish oil generated by the Maikop Group from that generated by the Diatom Formation. This study shows that these oils can be distinguished based on the distribution of specific biomarkers e.g. C_{30} steranes, C_{25} highly branched isoprenoids (HBIs), and the C_{25} isoprenoid pentamethylicosane (PMI).

INTRODUCTION

Onshore Azerbaijan is known for the presence of numerous oil and gas seeps. As self-ignition occurs frequently, Azerbaijan has become famous as the "land of eternal fire" and it has been suggested that the burning seeps formed the basis for the Zoroastrian religion (e.g. Selly and Sonnenberg, 2015). Oil seeps around Baku, the capital city, were described in the 13th century by Marco Polo; this area was the largest oil-producing region in the world during the second half of the 19th century and the early 20th century (e.g. Boote *et al*., 2018). Most oil production onshore Azerbaijan and in the South Caspian Sea comes from the Apsheron-Pribalkhan and the Lower Kura petroleum provinces (Boote *et al*., 2018; Fig. 1a). The main reservoirs are terminal fluvial fan sandstones of the Pliocene Productive Series (Hinds *et al*., 2004).

The Oligocene to middle Miocene Maikop Group and the upper Miocene Diatom Formation are generally considered to be the most important source rocks in this region, while older (e.g. Eocene) source units may also have contributed to the accumulation of hydrocarbons (e.g. Goodwin *et al*., 2020). In the offshore South Caspian Basin, these units are known to occur in the subsurface at depths of more than 10 km (Inan *et al*., 1997; Goodwin *et al*., 2020). However in onshore Azerbaijan, they are exposed at the surface in the Shamakhy-Gobustan area to the west of Baku (Fig. 1a) where outcropping source rocks have been the subject of detailed studies (TOC, Rock-Eval, organic geochemistry: Saint-Germès, 1998; Katz *et al*., 2000; Feyzullayev *et al*., 2001; Guliyev *et al*.,

2001; Saint-Germès *et al*., 2002; Hudson *et al*., 2008, 2016; Johnson *et al*., 2010; Bechtel *et al*., 2013; 2014; Alizadeh *et al*., 2017; Washburn *et al*., 2019). A synopsis of these studies suggests there is no consistent pattern in source rock data from the Maikop Group (Sachsenhofer *et al*., 2018a,b). For instance, it has been proposed that the highest quality source rock interval (~3 wt.% TOC; HI ~300 mgHC/gTOC) occurs in lower Oligocene units at Angeharan and Lahich (Bechtel *et al*., 2013, 2014: locations in Fig. 1a), whilst elevated TOC contents and HI values are also present in the upper Oligocene (TOC up to 4.7 wt.%; HI up to 350 mgHC/gTOC) and lower Miocene (TOC up to 5.8 wt.%; HI up to 400 mgHC/gTOC) at Siyaki and Khilmili, respectively (Saint-Germès 1998; see Fig. 1a for locations). Even higher TOC contents (max. 14.3 wt.%) and HI values (max. 800 mgHC/gTOC) were reported from a 14 m thick lower Miocene section at Gezdek (between Perekishkyul and Baku) by Katz *et al*. (2000).

Similarly, source rock parameters for the Diatom Formation vary greatly. TOC contents reported from outcrop samples are typically low (average 0.6 wt.%), but TOC contents up to 7.8 wt.% (average 1.0 wt.%) and HI values ranging from 107 to 807 mgHC/gTOC (average 308 mgHC/gTOC) occur in rock samples ejected from mud volcanoes (Isaksen *et al*., 2007), and in boreholes to the south of Baku (Alizadeh *et al*., 2017 and references therein). The low TOC contents in onshore samples were reproduced by Katz *et al*. (2000), Feyzullayev *et al*. (2001) and Johnson *et al*. (2010).

The lack of consistency indicates either major lateral and vertical variability in source-rock parameters, or issues surrounding the absolute chronology of the stratigraphy. Further problems are related to the general lack of integration of high-resolution (bio-)stratigraphy (e.g. Popov *et al*., 2008; Bati, 2015) and source rock studies. In this paper, to further the stratigraphic understanding of the Lower Kura Basin in Azerbaijan, we present representative source rock data from organic-rich intervals of Paleogene to late Miocene age from the Islamdag and Perekishkyul sections, located about 25 km NW of Baku (Fig. 1). The results offer new insights into the distribution of the main source rocks within the Eocene to Miocene sedimentary succession in eastern Azerbaijan and provide a basis for the identification of individual source rock intervals that may have generated hydrocarbons.

GEOLOGICAL SETTING

During Paleocene to Oligocene times, the territory of Azerbaijan evolved from being part of the northern Peri-Tethyan platform to being part of the Eastern Paratethys as a sea-level fall and intense tectonic activity separated the Paratethys from the World
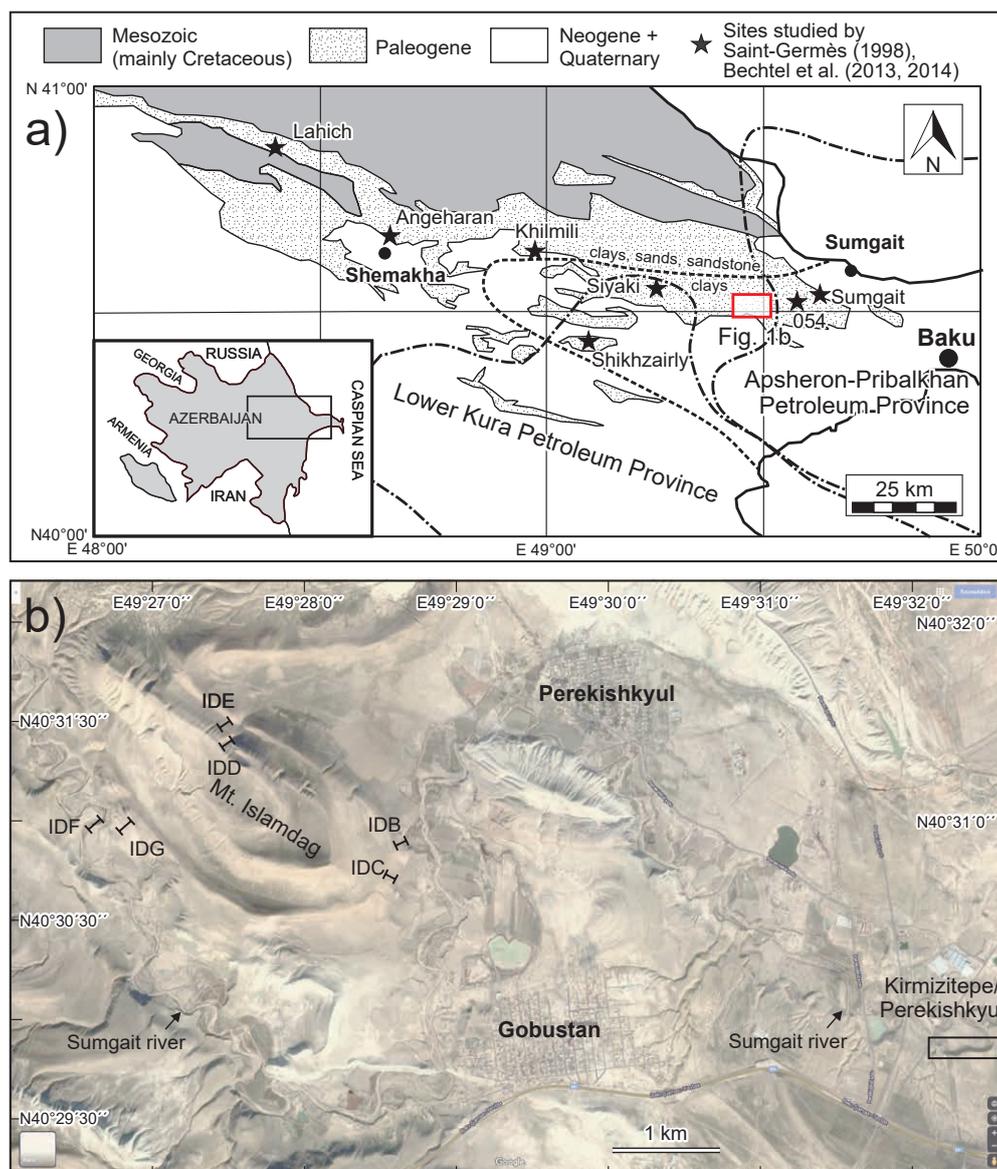
Fig. 1. (a) Simplified geological map of the Shamakhy-Gobustan area in eastern Azerbaijan with the general lithofacies of the Oligocene part of the Maikop Group in this area (Bechtel *et al.*, 2014). The boundaries of the Lower Kura and Apsheron-Pribalkhan petroleum provinces have been added (after Boote *et al.* , 2018).
(b) Google Earth image showing the study area with the location of the investigated sections. Sub-sections IDB to IDG constitute the "Islamdag section" of this paper.

ocean (Popov *et al*., 2004). Restriction of marine gateways before and after this separation caused two major episodes of oxygen-depleted conditions and the deposition of hydrocarbon source rocks during middle Eocene (Kuma Formation) and Oligocene to early Miocene times (Maikop Group; Sachsenhofer *et al*., 2018b). Basin restriction reached a peak during early Solenovian (mid-Rupelian) time (early NP23; ~31 Ma) and triggered Paratethys-wide low salinity conditions (Solenovian Event; Fig. 2) (e.g. Zaporozhets and Akhmetiev, 2015). The Solenovian Event is often characterized by a carbonate-rich layer (the Polbian or Ostracoda Bed; Gavrilov *et al*., 2017; Sachsenhofer *et al*., 2017, 2018a,b), but low salinity conditions continued during deposition of overlying carbonate-

free sediments. The Tarkhanian flooding event, recently dated as 14.85 Ma in the western Caucasus (Palcu *et al*., 2019b), terminated the anoxic conditions in the Eastern Paratethys. Thereafter marine environments with varying salinity conditions continued during middle and late Miocene time. A major (Pontian) transgression has been dated as 6.1 Ma (late Messinian; van Baak *et al*., 2016; 2017). In the South Caspian Basin, Miocene sediments are overlain by the fluvial lower Pliocene Productive Series (Hinds *et al*., 2004).

Cenozoic sediments in eastern Azerbaijan
The Cenozoic succession in eastern Azerbaijan is typically fine-grained and includes from base to top: the Paleocene Ilhidag and Sumgayit Formations, the
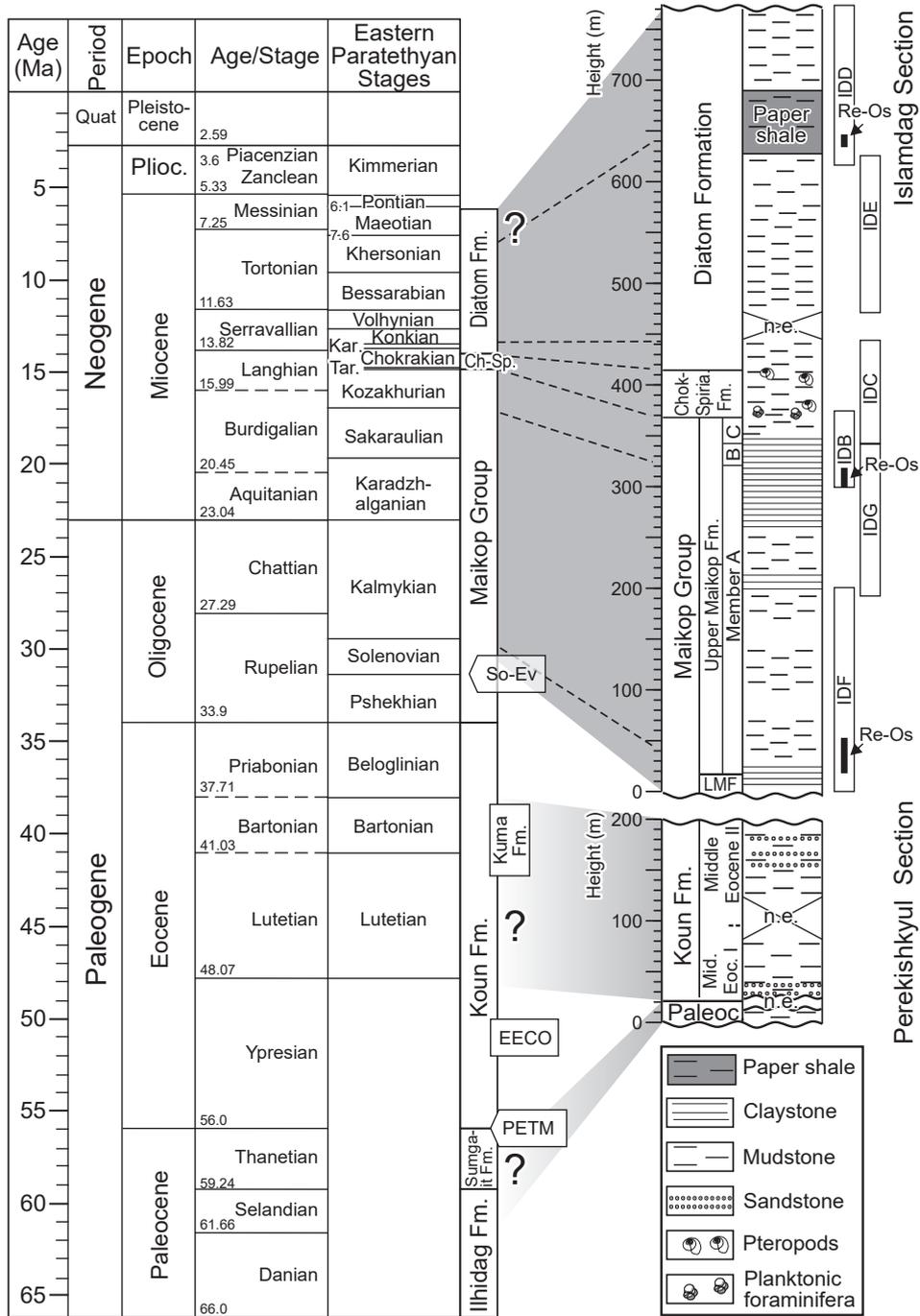
Fig. 2. Stratigraphic table with subdivisions and lithologies of Paleogene and Miocene sediments in the Perekishkyul and Islamdag sections. The time scale follows Gradstein *et al*. (2020). The subdivision of the Maikop Group in the Islamdag section and the ages of the Chokrak-Spirialis Formation and the basal Diatom Formation are based on Popov *et al*. (2008). IDF to IDD are the sub-sections studied in the Islamdag area. Black vertical bars in the IDF and IDD sections indicate the position of samples used for rhenium-osmium geochronology. (Re-Os samples in IDB are from Washburn *et al*., 2018, 2019). The age of the Paleocene/Eocene thermal maximum (PETM), the Early Eocene Climatic Optimum (EECO) and the Solenovian Event (So-Ev) are shown, together with the age of the Kuma Formation in the Caucasus area. n.e. – not exposed. Ch-Sp – Chokrak-Spirialis Formation.

Eocene Koun Formation, the Oligocene to middle Miocene Maikop Group, the Spirialis (= *Limacina* sp.; Pteropoda) Formation (termed the Chokrak-Spirialis Formation in this paper), and the middle to upper Miocene Diatom Formation (e.g. Johnson *et al*., 2010) (Fig. 2).

The Paleocene succession contains light brown, green and grey claystones with cm-scale siltstone intervals. The Eocene Koun Formation is dominated by light grey claystones, but includes reddish claystones in its middle part and dark grey beds near the top (Johnson *et al*., 2010).

Oligocene to middle Miocene sediments, attributed to the Maikop Group, are exposed along the flanks of Mount Islamdag (the "Islamdag section": Fig. 1b). The Maikop Group is dominated by laminated non-calcareous mudstones and claystones. These sediments have been studied previously using palynomorphs, calcareous phytoplankton and fish fossils (Popov *et al*., 2008) as well as rhenium-osmium (Re–Os) geochronology (Washburn *et al*., 2018; 2019). Whereas calcareous (benthic) fossils are largely absent, fish remains are common. Conventionally the Maikop Group in eastern Azerbaijan is divided into the Lower and Upper Maikop Formations, with the Upper Formation further separated into three lithological units, labelled from base to top as members A to C (Weber, 1935) (Fig. 2). Member A is the thickest unit and is rich in secondary jarosite on weathered surfaces in outcrops giving it a whitish to yellow colour in the field. Samples from the uppermost part of member A on the eastern slope of Mount Islamdag yielded a Re-Os age of 17.2 ± 3.2 Ma (Washburn *et al*., 2018; 2019). The age fits within the error range of the postulated early Miocene (Sakaraulian) age of the upper part of member A of the Maikop Group (Popov *et al*., 2008). Member B forms an important regional marker horizon and is composed of black, laminated non-calcareous mudstones with interbeds of platy siltstones (Popov *et al*., 2008). Member C is composed of laminated non-calcareous claystones to mudstones with jarosite weathering. Members B and C, characterized by impoverished endemic fish assemblages, may represent the Kozakhurian episode of salinity change. In terms of palaeogeography, the Maikop Group in eastern Azerbaijan represents deposition in one of the deepest parts of the Eastern Paratethys (Popov *et al*., 2008). Fish fossils indicate that oxygenated conditions extended down to a water depth of 600 m during early Miocene times (Akhmetiev *et al*., 2007).

The Chokrak-Spirialis Formation, weathering dark brown in outcrop, is composed of low-calcite claystones and calcareous claystones containing *Limacina* sp. planktonic microgastropods (Popov *et al*., 2008). The base of the interval with *Limacina* sp. is characterised by a distinct, light-grey marl bed rich in foraminifera (Weber, 1941). Dolostone interbeds up to 50 cm thick are commonly observed, particularly in the higher part of the unit. The average thickness of the formation in the study area is about 50 m. Based on the presence of carbonate components and the absence of jarosite in the Chokrak-Spirialis Formation, the boundary with the Maikop Group can readily be recognized in the field (Popov *et al*., 2008). The Chokrak-Spirialis Formation represents deposition during semi-marine conditions during Tarkhanian and early Chokrakian times (nannoplankton zones NN4-NN5; Akhmetiev *et al*., 2007).

Sediments of the Diatom Formation follow above those of the Chokrak-Spirialis Formation and contain multiple lithologically distinct units. The total thickness of the Diatom Formation varies greatly and can be in excess of 500 m. The basal part of the Diatom Formation is dated as Karaganian based on endemic fish fauna (e.g. *Sardinella karaganica*) implying a freshening phase compared to the underlying rocks (Popov *et al*., 2008). Higher in the Diatom Formation, which remains predominantly fine-grained, intervals with diatomites and organic-rich paper shale mudstones are found (Weber, 1941). Deposition of the Diatom Formation continued into late Miocene times (Johnson *et al*., 2010). This is further substantiated by the Diatom Formation being overlain by sediments dated as Pontian (late Messinian) elsewhere in the Gobustan region (van Baak *et al*., 2016; 2017).

Section descriptions
The Perekishkyul section
The Perekishkyul section, or sections referred to as Perekishkyul (including other spellings), have been described in the literature numerous times (Khalilov, 1962; Saint Germès, 1988; Saint Germès *et al*., 2002; Hudson *et al*., 2008, Johnson *et al*., 2010; Bati, 2015; Hudson *et al*., 2016). However, there is considerable uncertainty and/or inconsistency in the previous publications as regards the thickness of the section and the associated age model, and the precise location. In part, this is because exposures are common in the immediate vicinity of Perekishkyul village and range from Late Cretaceous to late Miocene in age. This makes the incorporation of these published datasets into the new results presented here highly ambiguous. Therefore, we prefer to limit the integration of data from previous papers when interpreting our work on the section.

The Perekishkyul section studied here (Figs 2, 3) comprises three main lithological intervals covering approximately 185 m true stratigraphic thickness. The base of the section is marked by a tight anticline with a prominent 1.2 m thick bed of bioclastic limestones. Bioclasts include planktic and benthic foraminifera, brachiopod spines, red algae and possible fragments of bryozoans and corals. The lowermost interval of relatively continuous exposure comprises 16 m of alternating beds of lighter and darker calcareous claystone/marls (Fig. 3b). Preliminary results from palynology and calcareous nannofossils suggests that these sediments were deposited during the Paleocene, although these data will be presented in more detail in a future paper.

The Paleocene section is overlain by a short interval (16-22 m) of highly deformed, dark grey calcareous mudstones, fractured marls/argillaceous limestones and red sheared mudstones, indicative of severe
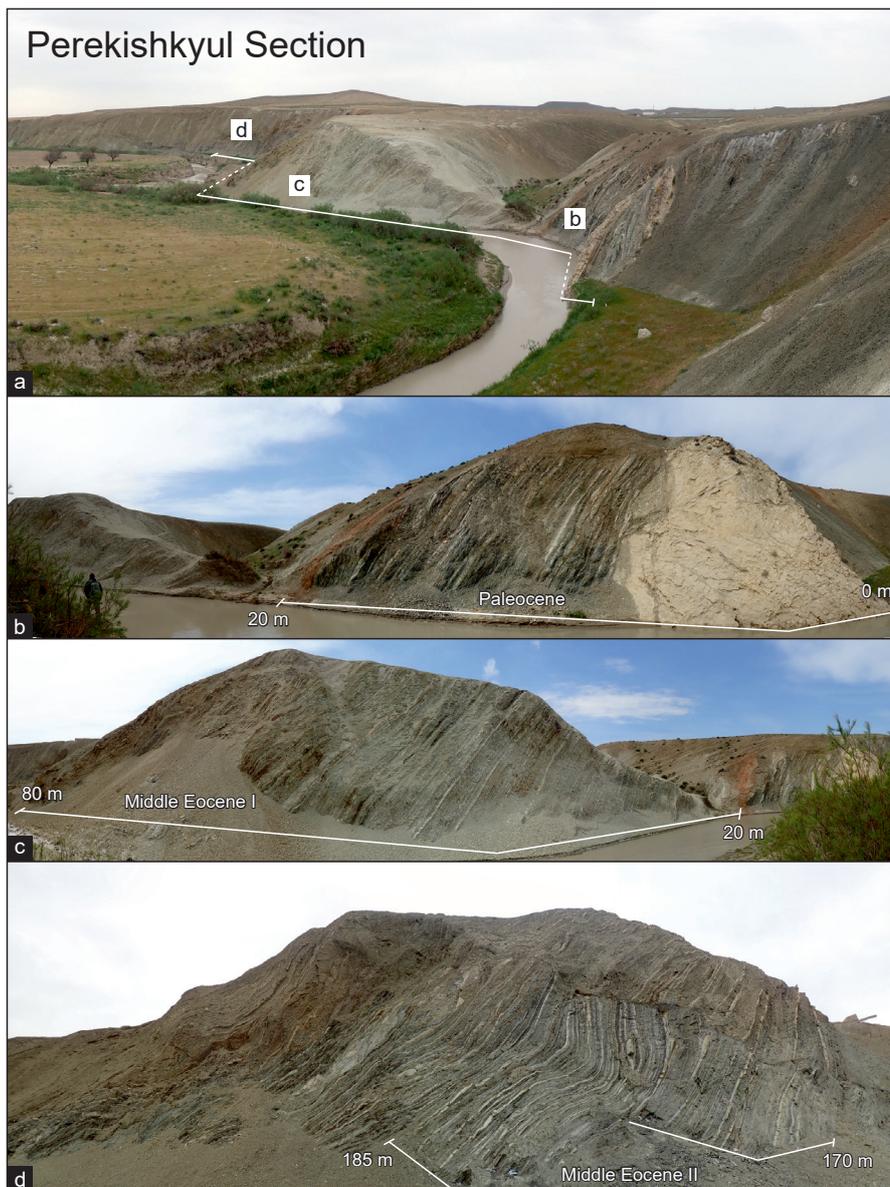
Fig. 3. Field photographs of the Perekishkyul section. (a) General view of the outcrop; (b, c, d) close-up views of particular intervals. (b) The Paleocene interval (0-20 m); (c) the lower part of the middle Eocene interval (Middle Eocene I; 20-80 m); (d) the upper part of the middle Eocene interval (Middle Eocene II; 175-185 m).

tectonic disturbance. The duration of missing time within this deformed interval is uncertain, but it likely accounts for a significant part of the latest Paleocene and early Eocene.

Overlying the deformed zone is a predominantly white-weathering interval attributed to the Eocene Koun Formation (22-81 m) which shows an alternation of two dominant claystone lithologies. The primary lithology is a recessive-weathering claystone which is typically non-calcareous. The second lithology comprises tabular and prominent claystone beds that retain some sedimentary structures such as ripples and lamination, as well as calcareous microfossils which are visible in hand specimen. A number of volcanic ash layers are also preserved within this part of the section. This interval contains dinoflagellates dated as Eocene (Bati, 2015). The age appears to be in line with

preliminary age data obtained by ^{40}Ar/^{39}Ar dating of ash layers, which suggest a middle Eocene age for the lower part of the interval. These data will be published in full in a future paper. Here, we refer to this part of the section as "Middle Eocene I" (Fig. 3c). Further logging upwards of this part of the section was not possible due to a gap in exposure.

Above the gap in exposure (81–134.5 m), two intervals were logged that were taken to be representative of the stratigraphically highest unit at Perekishkyul that represents a major lithological change compared to the underlying section. The lower of the two studied intervals in this topmost unit is predominantly composed of dark greenish grey, non-calcareous claystones. The higher interval (Fig. 3d) contains additional white calcareous marl interbeds up to 30 cm thick. A volcanic ash age in this part of the
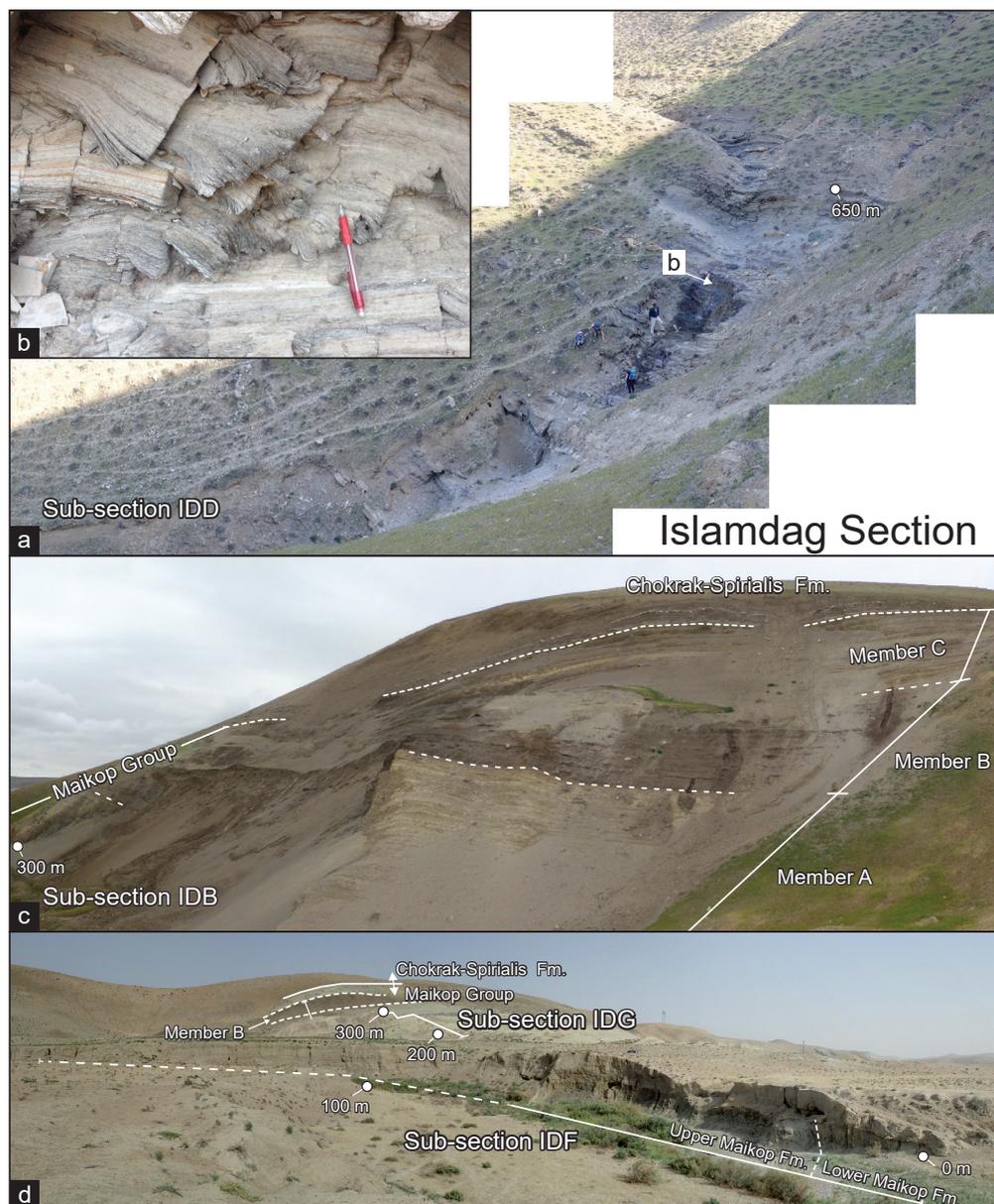
Fig. 4. Field photographs of the Islamdag section. (a) Sub-section IDD (paper shale); (b) close-up view of the paper shale; (c) sub-section IDB; (d) sub-sections IDF and IDG. See Fig. 1b for locations.

section suggests a depositional age at the end of the middle Eocene. We refer to these two stratigraphically highest intervals as "Middle Eocene II". Of particular importance in both intervals are cm-thick, black organic-rich non-calcareous claystone beds that appear to be interbedded with the background sediments. Overall, these black claystone beds may contribute up to 5 % of the total sediment thickness (probably less than 2 m net thickness) in the section.

The thicknesses of gaps in exposure have been estimated using average bedding orientations and GPS locations. The presence of chevron folding in the highest stratigraphic unit provides evidence of significant deformation, which reinforces the need for caution concerning the assumption of stratigraphic continuity. The thickness of the non-exposed sediments shown in Fig. 2 is therefore subject to a degree of uncertainty. Although exposures continue for several hundred metres further along the outcrop, the presence of folding and regular faulting may prevent a continuous section upwards from being established.

The Islamdag section

The Islamdag section (Figs 2, 4) exposes an apparently continuous succession of sedimentary rocks that are approximately 750 m thick. The lower 364 m of the section belong to the Maikop Group, with a basal 16 m of Lower Maikop Formation directly overlain by some 348 m of Upper Maikop Formation (Figs 2, 4d). Preliminary biostratigraphic data indicate that this part of the Lower Maikop Formation is significantly different from the Upper Maikop Formation, with common algae such as *Botryococcus braunii* and *Batiacasphaera* sp. indicating significantly reduced
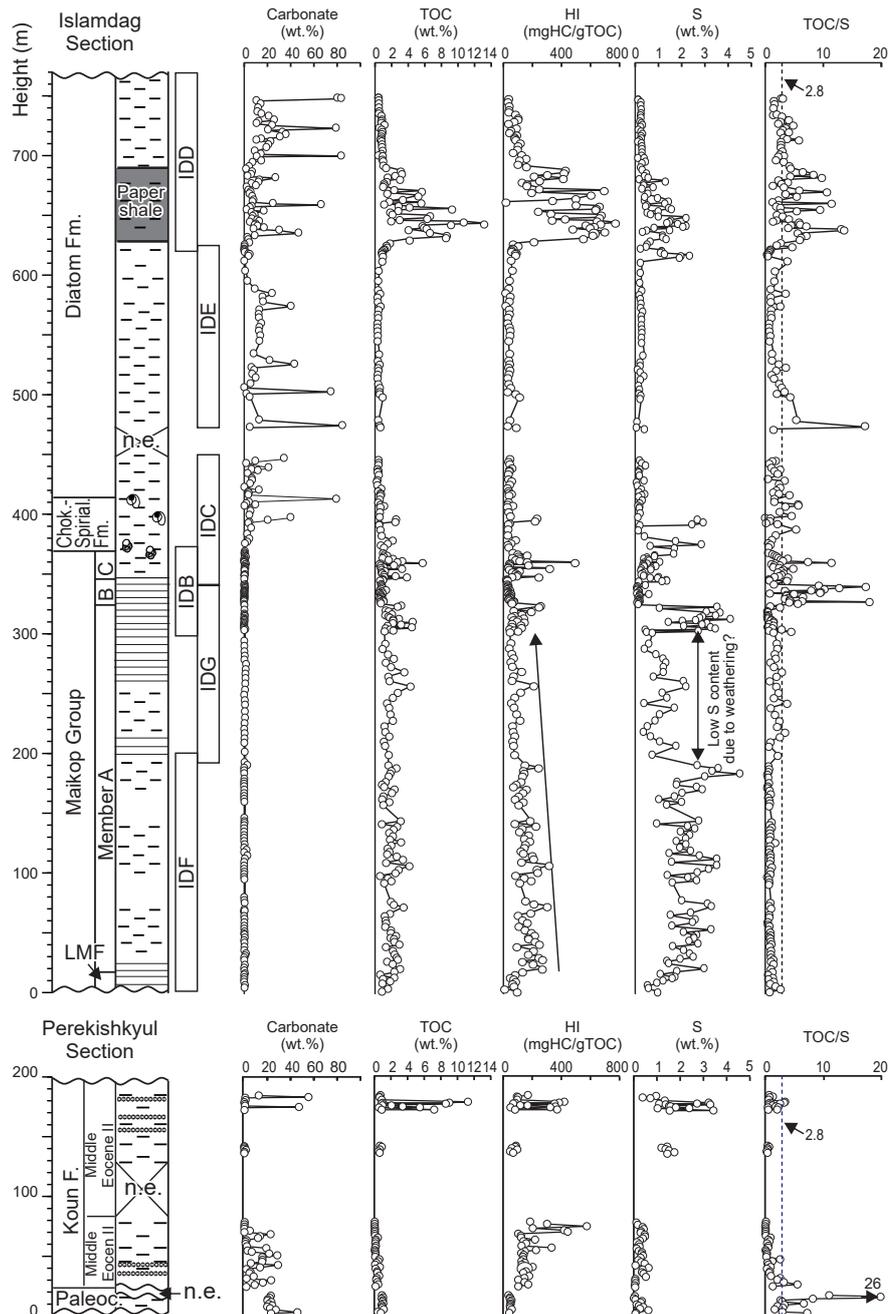
Fig. 5. Simplified lithological log of sediments exposed in the Perekishkyul and Islamdag sections together with carbonate contents and bulk geochemical parameters. TOC – Total Organic Carbon, HI – Hydrogen Index, S – Sulphur, n.e. – not exposed, LFM – Lower Maikop Formation. A TOC/S ratio of 2.8, characteristic of marine oxic environments (e.g. Berner, 1984), is indicated by the dashed line in the TOC/S versus depth plot.

salinities. This suggests correlation with the Rupelian Solenovian Event (Zaporozhets and Akhmetiev, 2015).

Within the Upper Maikop Formation, three lithologically distinct members can be identified (Figs 4c, 5): the members A (16–324 m), B (324–347 m) and C (347–364 m) of Weber (1935). The Maikop Group is predominantly composed of dark grey, non-calcareous laminated mudstones with yellow sulphur-rich jarosite alteration on weathered surfaces. Sandstones are rare throughout and, when present, occur as isolated cm-scale lenticular scour infills. The presence of diverse dinocysts with marine affinity in member A indicates

increased salinities compared to the underlying interval (Popov *et al*., 2008). Member B comprises dark grey, non-calcareous laminated mudstones with a brown oxidised appearance. Due to the change in weathering colour, this unit stands out in the field as a distinct, dark-coloured interval. *Batiacasphaera* sp. and *Botryococcus braunii* occur abundantly in this unit, suggesting a return to lower salinities (Popov *et al*., 2008). This reduction in salinity in the uppermost Maikop Group would suggest a correlation with the early Miocene Kozakhurian regional stage of the Eastern Paratethys.

The base of the overlying Chokrak-Spirialis Formation (368 m: Figs 4c, 5) is marked by a sharp transition to a 50 cm thick grey foraminifera marl. This point represents the first appearance of calcareous rocks and fossils. By correlation with other sections elsewhere in the Eastern Paratethys (Palcu *et al*., 2019b), this level likely has an age of 14.85 Ma. The overlying 47.5 m of the Chokrak-Spirialis Formation is composed of weakly calcareous laminated mudstones containing fossils of planktonic microgastropods. Occasional dolostone intervals up to 30 cm thick occur in this part of the section.

Overlying this, extending upwards to the top of the section, is the Diatom Formation which has a total stratigraphic thickness of ~330 m. The base of the Diatom Formation is gradational and is assigned an age of ca. 13.8 Ma, via correlation to the Karaganian regional stage of the Eastern Paratethys (Popov *et al*., 2008). The Diatom Formation is predominantly composed of a variety of fine-grained sediments comprising, from the base up: a >200 m thick interval dominated by diatomites and diatomaceous rocks with common dolostone interbeds (up to 550 m in the outcrop section); a mildly calcareous mudstone interval (550–610 m); a black non-calcareous mudstone reminiscent of the Maikop Group facies (610–625 m); bituminous paper shale calcareous mudstones (625–677 m; Fig. 4a,b); and an uppermost interval of weakly calcareous mudstones (677–750 m). The top of the section is interpreted as older than 6.1 Ma based on the absence of the lithologically and biostratigraphically distinct sediments of the younger Pontian regional stage (van Baak *et al*., 2016). Mineralogy and element concentrations of the interval between 613 and 663 m have been studied by Abdullayev *et al*. (2021; their Pereküşkül-Diatom section). Based on questionable correlations, the authors assumed a Karaganian to Konkian age for the interval.

SAMPLES AND METHODS

Samples
The present study focuses on samples from the Perekishkyul and Islamdag outcrop sections (Figs 3, 4). The Perekishkyul section (N40.49806° E 49.5355°) is located three kilometres east of the Perekishkyul settlement on the right bank of the Sumgait River (Fig. 1b) (e.g. Bati, 2015; his Kirmizitepe section) (Fig. 3). Sixty-seven samples were collected from ~200 m of stratigraphy encompassing the Paleocene-Eocene interval. The sampling interval in the studied parts of the section varied between 0.1 and 3.0 m.

At the Islamdag section, the Maikop Group as well as the overlying Chokrak-Spirialis and Diatom Formations were studied in six laterally-offset sub-sections located on the southwestern (N40.51628° E49.44321°), eastern (N40.51439° E49.47781°) and northeastern (N40.52461° E49.45959°) flanks of Mount Islamdag (cf. Popov *et al*., 2008). The sub-sections are labelled from base to top IDF, IDG, IDB, IDC, IDE and IDD (Figs 1b, 2, 4). Most adjacent sub-sections contain a significant overlap, but a gap between IDC and IDE is estimated to consist of roughly 22 m of stratigraphy based on GPS positions, bedding orientations and the general context in the field. In total, 300 samples were collected from ~750 m of section. The sampling interval varied between 0.3 and 6.0 m.

In order to minimize the effect of weathering, samples were collected from freshly exposed surfaces in hand-dug trenches up to 1 m deep. Nevertheless, the freshness of the sampled material depends on the initial exposure quality which varied significantly along the sections, and secondary effects on determined parameters cannot therefore be ruled out completely.

Methods
All samples were analyzed in duplicate for total sulphur (S), total carbon (TC) and total organic carbon (TOC; after acidification of samples) using an Eltra Helios C/S analyzer at Montanuniversitaet Leoben, Austria. The standard deviation of the C and S analyses were usually below 0.1 wt.%. This is in good agreement with the standard deviations of the standards used for calibration (e.g. S-standard: 2.27 % ± 0.06). The TC and TOC contents were used to calculate calcite equivalent percentages (Calc$_{equi}$ = [TC-TOC]*8.333).

A Rock-Eval 6 instrument was used to determine the amounts of free hydrocarbons (S1, mg hydrocarbons [HC]/g rock) and of hydrocarbons generated during thermal cracking (S2; mg HC/g rock). The hydrogen index (HI = 100*S2/TOC [mg HC/g TOC]) and the production index, PI = S1/(S1+S2), were calculated according to Espitalié *et al*. (1977). The temperature of maximum hydrocarbon generation (T$_{max}$) was recorded as a maturity parameter. The standard deviation of the Rock-Eval parameters S1 and S2 are below 0.07 and 0.5, respectively, which is in agreement with the results of the standards used (S1: 0.14 ± 0.07, S2: 12.43 ± 0.5). T$_{max}$ values show a standard deviation of 2°C at maximum.

In order to quantify the hydrocarbon potential of the potential source rock intervals, the amount of hydrocarbons which can be generated under a surface area of 1 m² was calculated using the Source Potential Index, SPI, which is defined as thickness*(S1 + S2)*bulk density/1000 (cf. Demaison and Huizinga, 1991).

Polished blocks were prepared for ten samples from the Perekishkyul section and 23 samples from the Islamdag section. Semi-quantitative maceral analysis used reflected white light and fluorescence light to distinguish aquatic macerals (e.g. alginite,

liptodetrinite) from terrestrial macerals (e.g. vitrinite, inertinite). Vitrinite reflectance measurements were performed using an incident light Leitz microscope following established procedures (Taylor *et al*., 1998). In addition, pyrite contents and fossil remains are described. Some of the samples were also investigated using scanning electron microscopy (Tescan Clara field emission SEM; see Misch *et al*., 2018 for details). To support the occurrence of diatoms, biogenic silica contents were quantified following a dissolution technique described by Zolitschka (1998).

Based on bulk geochemical parameters, 30 organic-rich samples (six middle Eocene samples from the Perekishkyul section; eleven samples from the Maikop Group; one sample from the Chokrak-Spirialis Formation and 12 samples of the Diatom Formation from the Islamdag section) were selected for organic geochemical analyses. Representative aliquots of selected samples were extracted for ca. 1 h using dichloromethane in a Dionex ASE 200 accelerated solvent extractor at 75°C and 100 bar. After evaporation of the solvent to 0.5 ml total solution in a Zymark TurboVap 500 closed cell concentrator, asphaltenes were precipitated from a hexane:dichloromethane solution (80:1 according to volume) and separated by centrifugation. The hexane-soluble fractions were separated into NSO compounds and aromatic and saturated hydrocarbons using medium pressure liquid chromatography with a Köhnen-Willsch instrument (Radke *et al*., 1980). The hydrocarbon fractions were analysed by a gas chromatograph equipped with a 60 m DB-5MS fused silica capillary column (0.25 µm film thickness) coupled to a ThermoFisher ISQ mass spectrometer. The oven temperature was programmed from 40°C to 310°C at 4°C/min, followed by an isothermal period of 30 min. Helium was used as the carrier gas. The sample was injected splitless at an injector temperature of 275°C. The spectrometer was operated in the EI (electron ionization) mode over a scan range from mass-to-charge ratio (*m/z*) 50 to *m/z* 650 (0.7 s total scan time). Individual compounds were identified on the basis of retention time in the total ion current (TIC) chromatogram and by comparison of the mass spectra with published reference data. Identification of pentamethylicosane (PMI) is based on abundant mass fragments 239 and 267, and the presence of irregular PMI was indicated by *m/z* 239 > 253. The C_{25} highly branched isoprenoid (HBI) alkane and thiophenes were identified by diagnostic fragments 238 and 265, respectively. Absolute concentrations of most compounds were calculated using peak areas in the TIC chromatograms in relation to those of internal standards (squalane and 1,1′-binaphthyl). Compounds present in insufficient intensities for peak integration in the TIC (e.g. steranes, sterenes and hopanoids) were quantified by integration of

peak areas in appropriate mass chromatograms using response factors to correct for the intensities of the fragment ion used for quantification of the total ion abundances. The concentrations were normalized to TOC. The uncertainties in concentrations are in the range of 5 to 10% (relative error), the latter resulting from peaks of low intensities.

Stable carbon isotope measurements of specific compounds were performed on selected samples using a Trace GC instrument coupled to a ThermoFisher DELTA-V IR mass spectrometer via a GC isolink combustion interface. CO_2 was injected during each analysis as a monitoring gas. The GC column and temperature programme used were the same as above. The samples, saturated and aromatic hydrocarbon fractions, were placed into tinfoil boats for the bulk carbon isotope analyses and combusted in an oxygen atmosphere using an elemental analyser (Flash EA 1112) at 1020 °C. The evolving CO_2 was separated by column chromatography and analysed online using a DELTA-V IR-MS. The $^{13}C/^{12}C$ isotope ratios of CO_2 were compared with the monitoring gas. Stable isotope ratios are expressed relative to the Vienna Pee Dee Belemnite (V-PDB) standard in delta notation ($\delta^{13}C = [(\delta^{13}C/\delta^{12}C)_{sample}/(\delta^{13}C/\delta^{12}C)_{standard} - 1]$; Coplen, 2011). Delta notation is reported in parts per thousand or per mil (‰). The analytical error during the measurements was in the range of 0.2‰ to 0.3‰.

Samples for rhenium-osmium (Re-Os) geochronology were taken from the organic-rich (1.2-10.8 wt.% TOC) lower part of the Maikop Group (16 samples: IDF-09-24; 18.0-53.1 m) in the Islamdag section, and from the paper shale interval in the Diatom Formation (9 samples: IDD-13-19 and IDD-21-23; 633.4-646.5 m; Fig. 2). The large sampling interval was not considered to be a problem, as Washburn *et al*. (2019) observed relatively similar Re-Os values over several metres of stratigraphy. The selected samples were polished with silica carbide grit pads to minimize weathering effects and to remove any contamination by metal tools. Samples were then powdered in an alumina-ceramic shatterbox to yield 30-80 g of powdered sample. The Re-Os analysis was conducted at the Laboratory for Sulfide and Source Rock Geochemistry and Geochronology, and the Arthur Holmes Laboratory, Durham University. Each shale aliquot was dissolved in ~8 mL of 0.25g/g of CrO_3 in $4N\ H_2SO_4$ with a known amount of $^{185}Re+^{190}Os$ tracer (spike) solution at 220ºC for 48 hr. The Re-Os laboratory protocol follows that described in Selby and Creaser (2003) and Cumming *et al*. (2013). The Re and Os isotopic compositions were determined using negative thermal ionization mass spectrometry (NTIMS) using a Thermo Scientific Triton mass spectrometer (Völkening *et al*., 1991; Creaser *et al*., 1991). The running average of the isotopic
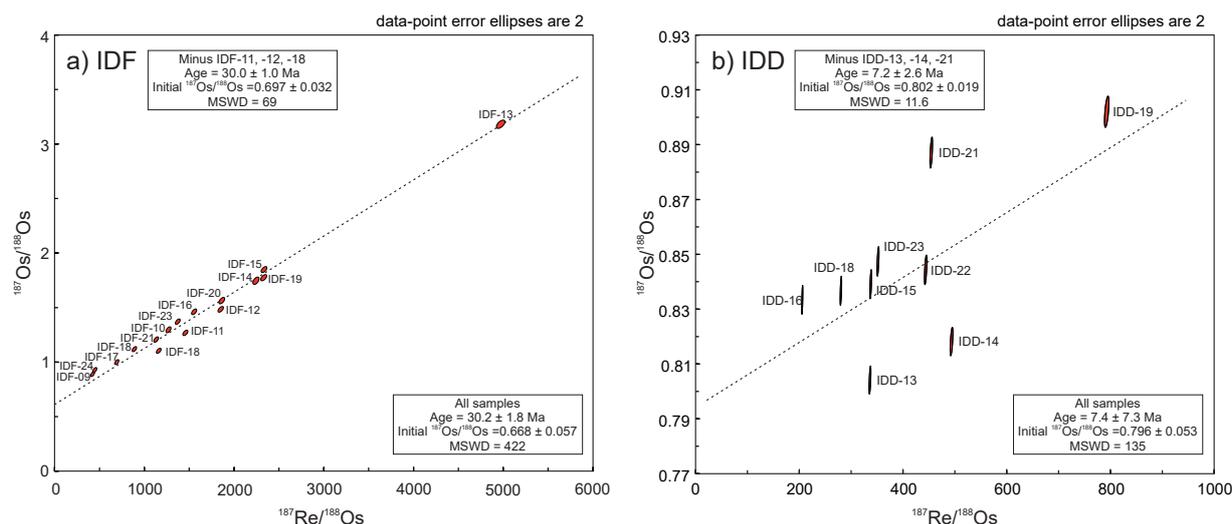
Fig. 6. (a) ^{187}Re/^{188}Os versus ^{187}Os/^{188}Os plot for the IDF sub-section at the Islamdag section. **(b)** ^{187}Re/^{188}Os versus ^{187}Os/^{188}Os plot for the IDD sub-section of the paper shale interval in the Diatom Suite. See text for details and discussion.

compositions of in-house Re and Os standard solutions are 0.59863 ± 0.00203 (N = 495) for ^{185}Re/^{187}Re (ReStd 125 pg solution) and 0.16087 ± 0.0004 (N = 513) for ^{187}Os/^{188}Os (DROsS 50 pg solution). The total procedural blank for Re and Os are 0.10 ± 0.5 pg and 16.0 ± 1.0 pg, respectively, with a ^{187}Os/^{188}Os of 0.20 ± 0.05 (n =4). The Re-Os isotopic data including 2σ calculated uncertainties for ^{187}Re/^{188}Os and ^{187}Os/^{188}Os and the associated error correlation function (rho; Ludwig, 1980) were regressed using IIsochron program Isoplot (Ludwig, 2011) and IsoplotR (Vermeesch, 2018) using the ^{187}Re decay constant of $1.666e-11 \pm 5.165-14a-1$ (Smoliar *et al.*, 1996).

RESULTS

Rhenium-osmium geochronology

The sample suite from the basal part (18.0-53.1 m) of member A (IDF sub-section) in the Islamdag section (1.2-2.9 wt.%TOC) has Re and Os abundances between 3.4 and 281.4 ppb and 44.7 and 383.7 (^{192}Os = 16.7-113.1) ppt, respectively (Table 1). The ^{187}Re/^{188}Os and ^{187}Os/^{188}Os compositions range between 402.5 and 4951.3, and 0.912 and 3.203 (Table 1), and are positively correlated. Linear regression using Isoplot v.4.15 of the ^{187}Re/^{188}Os and ^{187}Os/^{188}Os data for the entire sample set yielded a Model 3 Re-Os date of 30.2 ± 1.8 Ma, with an initial ^{187}Os/^{188}Os of 0.668 ± 0.057 (Mean Squared Weighted Deviates [MSWD] = 422; Fig. 6a). The Model 3 regression and MSWD >1 indicate that the scatter about the best-fit line of the Re-Os data is beyond that described by analytical uncertainties, and is controlled by a normal distributed variation in the initial ^{187}Os/^{188}Os of 0.120 (2σ) (Ludwig, 2011) or a non-normal variation in the initial ^{187}Os/^{188}Os of between 0.040 and 0.081 (2σ) (IsoplotR; Vermeesch, 2018). The scatter about the best-fit line

is mainly caused by three samples (IDF-11, IDF-12, IDF-18), which possess initial ^{187}Os/^{188}Os at 30 Ma of between 0.56 and 0.59 (Table 1) and exhibit between 5.2 and 9.3% deviation from the line of best-fit. Linear regression of the Re-Os data set without samples IDF-11, -12 and -18 exhibits significantly less scatter (MSWD = 69), yet yielded an identical Re-Os date (30.0 ± 1.0 Ma, ^{187}Os/^{188}Os = 0.70 ± 0.03) (Fig. 6a). The scatter about the best-fit line is a result of a normal distributed or non-normal variation in the ^{187}Os/^{188}Os of 0.061 (Isoplot, Ludwig, 2011) or 0.0195 to 0.0435 (IsoplotR, Vermeesch, 2018), respectively. The Re-Os date indicates a late Rupelian (Solenovian) depositional age for the base of the Islamdag section. The initial ^{187}Os/^{188}Os of 0.70 ± 0.03 is higher (contains more radiogenic ^{187}Os) than that of the contemporaneous global ocean (Peucker-Ehrenbrink and Ravizza, 2020).

The samples from the IDD sub-section of the paper shale of the Diatom Formation (633.4-646.5 m; 1.8-10.8 wt.%TOC) in the upper part of the Islamdag section possess Re and Os abundances of 6.4 to 23.6 ppb and 127.9 to 261.8 (^{192}Os = 48.3 – 99.3) ppt, respectively (Table 1). The ^{187}Re/^{188}Os and ^{187}Os/^{188}Os compositions range between 205.3 and 793.2, and 0.804 and 0.902 (Table 1). The ^{187}Re/^{188}Os and ^{187}Os/^{188}Os data exhibit significant scatter about a best-fit line (Re-Os date = 7.4 ± 7.3 Ma, initial ^{187}Os/^{188}Os of 0.796 ± 0.053, MSWD = 135) (Fig. 6b). The scatter about the best-fit line is a result of a normal distributed or non-normal variation in the ^{187}Os/^{188}Os of 0.049 (Isoplot, Ludwig, 2011) or 0.014 to 0.029 (IsoplotR, Vermeesch, 2018), respectively. The scatter about the best-fit line is caused by three samples (IDD-13, 14, 21). Without these samples a Model 3 Re-Os date of 7.2 ± 2.6 Ma and an initial ^{187}Os/^{188}Os of 0.80 ± 0.02 (MSWD = 12) is obtained (Fig. 6b). The scatter is explained by normal distributed variation in the ^{187}Os/^{188}Os of

Table 1. Sample dates from Re-Os isochron analysis.

Sample ID	Stratigraphic height (m)	Re (ppb)	± 2 s.e.	Os (ppt)	± 2 s.e.	192Os (ppt)	± 2 s.e.	187Re/188Os	± 2 s.e.	187Os/188Os	± 2 s.e.	rho	% Re Blank	% 187Os Blank	% 188Os Blank	Osi @ 7.2 myr	±
Paper Shale																	
IDD-23	646.45	8.5	0.0	127.9	0.5	48.3	0.2	351.6	1.6	0.848	0.004	0.593	0.19	0.02	0.07	0.805	0.004
IDD-22	645.45	16.5	0.0	196.5	0.7	74.2	0.3	443.4	1.9	0.844	0.004	0.584	0.10	0.01	0.04	0.791	0.004
IDD-21	644.75	14.8	0.0	172.0	0.6	64.6	0.2	454.3	2.0	0.887	0.005	0.590	0.11	0.01	0.05	0.833	0.005
IDD-19	642.25	23.6	0.1	157.8	0.6	59.1	0.2	793.2	3.5	0.902	0.005	0.591	0.07	0.01	0.05	0.807	0.005
IDD-18	641.45	7.4	0.0	139.1	0.5	52.6	0.2	279.9	1.2	0.837	0.004	0.592	0.22	0.01	0.06	0.803	0.004
IDD-16	639.15	6.4	0.0	164.6	0.6	62.2	0.2	205.3	0.9	0.833	0.004	0.587	0.25	0.01	0.05	0.809	0.004
IDD-15	638.05	10.5	0.0	163.2	0.6	61.6	0.2	337.5	1.5	0.839	0.004	0.589	0.15	0.01	0.05	0.799	0.004
IDD-14	635.65	19.0	0.0	202.2	0.7	76.6	0.3	493.5	2.2	0.818	0.004	0.588	0.08	0.01	0.04	0.759	0.004
IDD-13	633.45	16.8	0.0	261.8	0.9	99.3	0.4	336.1	1.5	0.804	0.004	0.584	0.10	0.01	0.03	0.764	0.004
Base of Member A																**Osi @ 30 myr**	
IDF-24	53.10	19.5	0.0	244.8	0.9	91.3	0.3	425.5	1.9	0.949	0.005	0.573	0.08	0.01	0.04	0.736	0.010
IDF-23	50.85	50.4	0.1	209.5	0.9	74.2	0.3	1351.1	5.9	1.392	0.007	0.590	0.03	0.00	0.02	0.717	0.007
IDF-22	48.40	48.9	0.1	307.1	1.2	112.0	0.4	867.6	3.8	1.140	0.006	0.586	0.03	0.00	0.01	0.706	0.006
IDF-21	46.75	45.8	0.1	227.3	0.9	82.1	0.3	1110.2	4.9	1.228	0.006	0.589	0.04	0.00	0.02	0.673	0.007
IDF-20	45.80	80.1	0.2	249.3	1.3	86.5	0.4	1841.8	9.5	1.585	0.011	0.585	0.02	0.00	0.02	0.664	0.011
IDF-19	43.40	67.5	0.2	171.4	0.8	58.1	0.2	2309.7	10.6	1.795	0.010	0.589	0.02	0.00	0.03	0.641	0.011
IDF-18	41.10	64.0	0.2	306.2	1.2	111.8	0.4	1138.5	4.9	1.125	0.006	0.580	0.05	0.01	0.06	0.556	0.010
IDF-17	39.00	10.6	0.0	85.2	0.3	31.5	0.1	670.9	3.1	1.021	0.005	0.608	0.16	0.01	0.05	0.686	0.006
IDF-16	35.70	63.2	0.2	233.7	1.0	82.0	0.3	1534.0	6.7	1.483	0.008	0.588	0.03	0.00	0.02	0.716	0.008
IDF-15	32.70	95.7	0.2	244.7	1.1	82.3	0.3	2313.3	10.0	1.870	0.009	0.584	0.03	0.01	0.08	0.713	0.010
IDF-14	30.05	101.9	0.2	268.0	1.6	91.1	0.4	2223.5	12.0	1.768	0.014	0.539	0.03	0.01	0.07	0.656	0.010
IDF-13	28.30	281.4	0.7	383.7	2.2	113.1	0.4	4951.3	22.3	3.203	0.017	0.587	0.01	0.00	0.06	0.728	0.023
IDF-12	26.65	44.2	0.1	137.4	0.6	48.1	0.2	1830.5	8.1	1.505	0.008	0.596	0.04	0.01	0.03	0.590	0.008
IDF-11	24.60	81.3	0.2	314.5	1.3	112.8	0.4	1434.9	6.4	1.289	0.007	0.564	0.02	0.00	0.01	0.572	0.007
IDF-10	20.40	44.0	0.1	196.2	0.9	70.1	0.3	1247.6	6.0	1.318	0.009	0.543	0.04	0.00	0.02	0.694	0.009
IDF-09	18.00	3.4	0.0	44.7	0.2	16.7	0.1	402.5	2.0	0.912	0.005	0.643	0.49	0.03	0.10	0.711	0.005

Formation groups (left margin labels): Diatom Formation; Maikop Group

Fig. 7. Cross-plots of Rock-Eval T$_{max}$ versus hydrogen index (HI), and TOC versus Rock-Eval S2, for different stratigraphic units in the Islamdag section (top panel) and the Perekishkyul section (bottom panel). The plots show that the paper shales in the Diatom Formation and organic-rich layers in the Koun Formation (Middle Eocene II) (Perekishkyul section) contain Type II kerogen, whereas kerogen Type III is dominant in the remaining units. Fm: Formation.
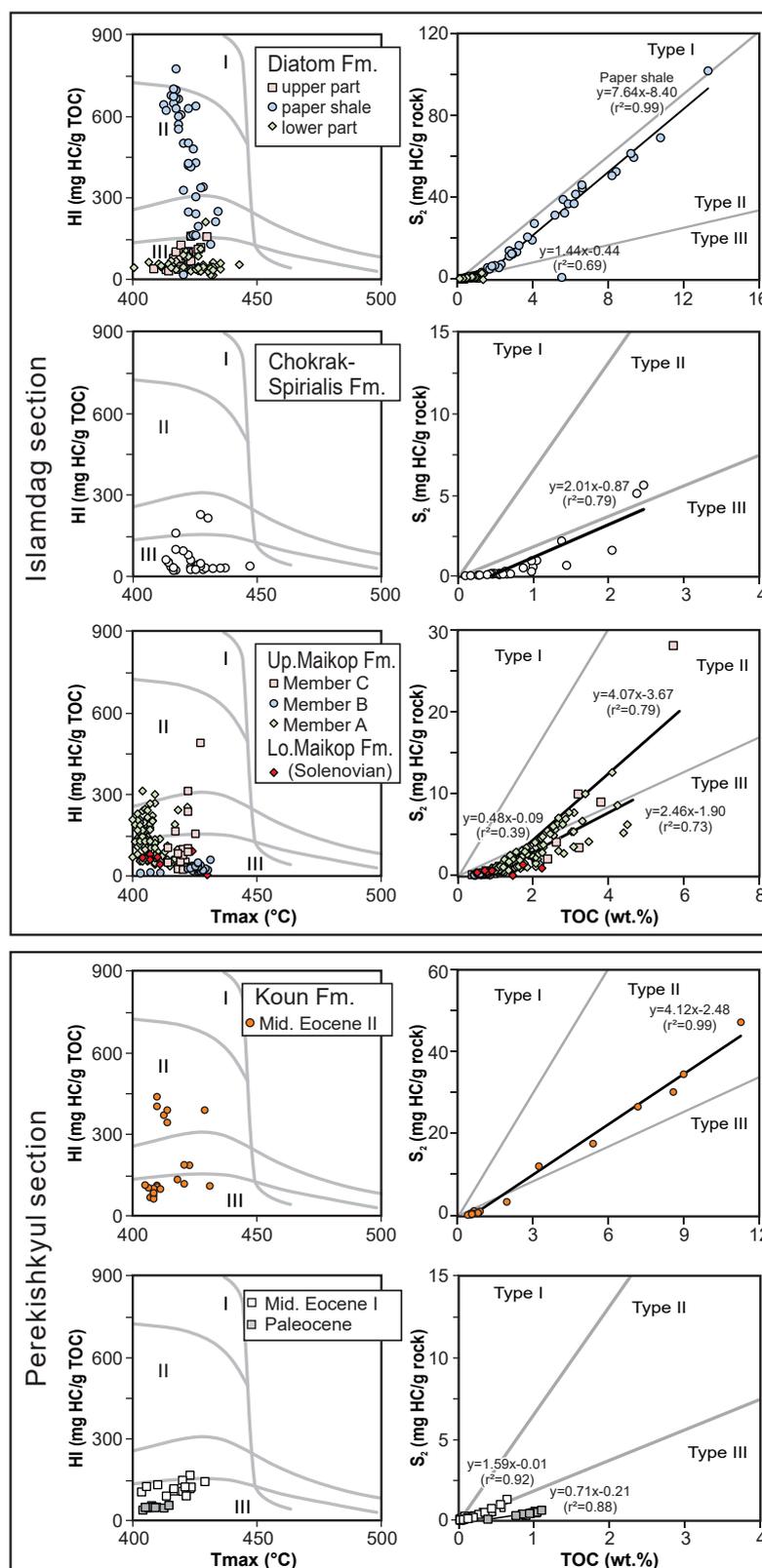
0.014 (Ludwig, 2011) or a non-normal variation in the [187]Os/[188]Os of 0.0031 to 0.0118 (Vermeesch, 2018), with sample IDD-22 showing the largest deviation (1.3 %) from the best-fit line.

The Re-Os date indicates a late Tortonian/early Messinian depositional age for the paper shale interval in the Diatom Formation. The initial [187]Os/[188]Os of 0.80 ± 0.02 is slightly lower than the trend observed in the late Miocene global [187]Os/[188]Os oceanic values (Peucker-Ehrenbrink and Ravizza, 2020).

Bulk geochemical parameters
Stratigraphic plots of bulk geochemical parameters are presented in Fig. 5. Cross-plots of T$_{max}$ versus

Table 2. Average, minimum and maximum values of bulk geochemical parameters for samples from different stratigraphic units in the Islamdag and Perekishkyul sections.

				TOC (wt.%)	Calcite equiv. (wt.%)	S (wt.%)	TOC/S (--)	S1 mgHC/ g rock	S2 mgHC/ g rock	HI mgHC/ gTOC	Tmax (°C)
Islamdag Section		Diatom Formation	**688-750 m**								
			max	1.23	83.48	0.42	5.83	0.07	1.90	154	429
			avg	0.64	25.03	0.23	2.93	0.03	0.51	76	419
			min	0.30	1.59	0.09	1.43	0.01	0.06	26	394
			Paper shale (629-688 m)								
			max	13.27	66.14	2.20	13.62	3.04	102.03	770	434
			avg	4.35	11.84	0.96	5.24	0.55	23.98	456	421
			min	0.87	2.04	0.15	1.28	0.03	0.64	12	412
			429-629 m								
			max	1.08	84.45	2.35	17.21	0.07	0.93	107	444
			avg	0.43	12.84	0.41	2.00	0.02	0.23	44	423
			min	0.17	0.00	0.03	0.36	0.01	0.04	10	373
	Maikop Group	Chokrak-Spirialis Fm	**364-429 m**								
			max	2.46	79.00	2.95	5.70	0.34	5.60	227	447
			avg	0.81	8.08	0.78	2.25	0.06	0.76	60	424
			min	0.09	0.00	0.03	0.20	0.01	0.05	22	413
		Upper Maikop Formation	**Member C (347-364 m)**								
			max	5.72	1.51	1.05	11.43	2.44	28.11	491	427
			avg	1.71	0.48	0.52	3.26	0.26	3.30	114	420
			min	0.39	0.00	0.22	1.08	0.02	0.14	28	414
			Member B (325-347 m)								
			max	1.22	0.71	1.36	18.00	0.04	0.62	67	431
			avg	0.69	0.14	0.28	6.04	0.02	0.25	35	424
			min	0.43	0.00	0.04	0.63	0.02	0.11	15	403
			Member A (16-324 m)								
			max	4.49	2.76	4.55	4.50	0.39	12.71	311	425
			avg	1.88	0.28	2.00	1.18	0.11	2.69	126	407
			min	0.49	0.00	0.29	0.36	0.02	0.28	29	395
		Lo.Maikop Formation	**0-16 m**								
			max	2.23	0.67	1.71	2.64	0.09	1.37	90	430
			avg	1.15	0.25	1.06	1.22	0.04	0.63	60	413
			min	0.52	0.00	0.51	0.49	0.01	0.04	3	404
Perekishkyul Section	Koun Fm.	Middle Eocene II	**179-184 m**								
			max	0.87	55.33	1.36	1.34	0.05	1.19	169	423
			avg	0.68	17.14	0.88	0.87	0.03	0.78	115	415
			min	0.56	0.83	0.41	0.64	0.01	0.52	93	407
			171-178 m (organic-poor layers)								
			max	0.99	0.67	1.57	0.88	0.05	1.10	117	413
			avg	0.83	0.13	1.34	0.63	0.04	0.69	79	407
			min	0.53	0.00	1.05	0.50	0.03	0.26	50	405
			171-178 m (organic-rich intercalations)								
			max	11.26	30.00	3.44	3.47	0.61	47.26	420	421
			avg	6.67	4.46	2.59	2.47	0.36	24.56	342	411
			min	2.00	0.00	1.40	1.24	0.07	3.41	171	407
			135-142 m								
			max	0.86	1.34	1.77	0.71	0.03	0.71	96	408
			avg	0.64	0.23	1.48	0.45	0.03	0.48	73	406
			min	0.46	0.00	1.22	0.26	0.02	0.21	46	404
		Middle Eocene I	**23-78 m**								
			max	0.64	29.09	0.67	5.61	2.00	1.30	575	426
			avg	0.19	9.20	0.31	0.88	0.02	0.30	186	413
			min	0.02	0.05	0.08	0.04	0.00	0.04	102	394
		Paleocene	**0-16 m**								
			max	1.10	45.77	0.66	26.19	0.05	0.64	58	412
			avg	0.90	24.28	0.25	6.54	0.04	0.42	46	405
			min	0.39	19.73	0.04	1.67	0.03	0.10	26	395

Abbreviations:
TOC – total organic carbon; S – sulphur; S1 – amount of free hydrocarbons;
S2 – amount of generated hydrocarbons; min – minimum; avg – average;
max – maximum; T_{max} - temperature of maximum hydrocarbon generation.

hydrogen index (HI) and TOC versus S_2 are shown in Fig. 7. Average, minimum and maximum values of bulk geochemical parameters for each stratigraphic unit are listed in Table 2.

The Perekishkyul section
The average TOC and sulphur contents of the Paleocene interval are 0.90 and 0.25 wt.%, respectively. The sulphur content is low in the two lowermost samples and shows a general decrease upwards in the remaining part of the section. Apart from the basal layers, TOC/S ratios generally increase upward from 1.7 to 26.2 (Fig. 5). HI (26-58 mgHC/gTOC), T_{max} (395-412°C; Table 2) and PI (<0.1) are low.

Samples from the Middle Eocene I interval contain small amounts of organic matter (0.02-0.64

wt.% TOC) and sulphur (0.08-0.67 wt.% S). A very low TOC content (<0.05 wt.%) occurs in samples from the upper 10 m of this section. TOC/S ratios show a general decrease upwards from 5.6 to 0.09. HI values are slightly higher than in the Paleocene section and typically range from 100 to 200 mgHC/gTOC. Even higher values (up to 575 mgHC/gTOC) are found in samples with a TOC content below 0.2 wt.% and high PI values (>0.1). Hence, these data probably reflect contamination. T_{max} values could be determined reliably only for samples with relatively high TOC contents, and are of the same order as those of samples from the Paleocene interval (394-426°C).

Whereas the TOC content is below 1.0 wt.% in most Middle Eocene II samples, significantly higher values (2.0-11.4 wt.%) are observed in thin black shales within the upper part of the exposed section. The sulphur content of organic-lean sediments ranges from 0.6 to 1.8 wt.%, whereas that in organic-rich sediments varies between 1.6 and 3.5 wt.%. TOC/S ratios increase with increasing TOC contents and reach a maximum of 3.5 in a sample with 11.3 wt.% TOC. HI values are below 200 mgHC/gTOC in samples with low or moderate TOC contents (<2.1 wt.%), but vary between 323 and 420 mgHC/gTOC in samples with high TOC contents (3.4-11.3 wt.%).

The Islamdag section
The Lower Maikop Formation (0-16 m) in the Islamdag section contains moderate amounts of organic matter (avg. 1.15 wt.% TOC) with very low HI values (avg. 60 mgHC/gTOC). The sulphur content (avg. 1.06 wt.%) increases upwards and TOC/S ratios (avg. 1.22) decrease in the same direction.

Bulk geochemical parameters of the Upper Maikop Formation vary significantly for samples from members A to C. The TOC content in member A is moderately high (average: 1.88 wt.%; max. 4.49 wt.%). Sulphur contents in sub-section IDF (16-191 m) are on average 2.33 wt.%. The rocks have a very low TOC/S ratio (avg. 0.82). Significantly lower sulphur contents (avg. 0.96 wt.%) and higher TOC/S ratios (average: 1.89) were obtained for IDG samples (199-339 m). This is likely the result of more intense weathering on this slope exposure compared to the river bed exposures in sub-section IDF. Sulphur contents (avg.: 2.59 wt.%) and TOC/S ratios (avg. 1.21) of member A samples from sub-section IDB (302-325 m) are similar to those in samples from sub-section IDF. HI values are on average 126 mgHC/gTOC (max. 311 mgHC/gTOC). They show a gradual decrease between 16 and 300 m, followed by an increase up-section.

The black-coloured member B has surprisingly low values of TOC (avg. 0.69 wt.%), HI (avg. 35 mgHC/gTOC) and sulphur content (avg. 0.28 wt.%), but a high average TOC/S ratio of 6.04. The overlying member C

contains on average 1.71 wt.% TOC (max. 5.72 wt.%) and 0.52 wt.% sulphur. TOC/S ratios are relatively high (avg. 3.30). HI values (avg. 114 mgHC/gTOC) between 200 and 491 mgHC/TOC were determined for three samples. The average T_{max} of the Maikopian samples in the Islamdag section is 412°C. PI values increase upwards from around 0.03 to 0.10.

The Chokrak-Spirialis Formation typically contains low amounts of organic matter (avg. TOC: 0.82%) and has a low HI value (avg. 58 mgHC/gTOC). However, the formation includes a number of thin (~30 cm), microgastropod-bearing laminated mudstones, two of which (samples IDC-48.2 and IDC-48.4) have been included in the present study. These mudstones have high TOC contents (2.37 and 2.46 wt.%) and have moderately high HI values (214 and 227 mgHC/gTOC). The sulphur content varies widely from 0.10 to 2.95 wt.%, and maximum values occur in organic-rich samples. TOC/S ratios in these samples are below 1.0, but are significantly higher (up to 5.73) in low-TOC samples. The average TOC/S ratio and the average T_{max} are 2.67 and 423°C, respectively. PI values range from 0.02 to 0.26 for the entire samples set and from 0.02 to 0.19 for samples with a TOC content exceeding 1 wt.%.

Data for samples from the Diatom Formation are presented separately for sediments below the paper shales (429-629 m), the paper shale interval itself (629-688 m), and for the overlying sediments (688-749 m; Table 2). Sediments below the paper shale have low TOC (avg. 0.42 wt.%) and low sulphur contents (avg. 0.35 wt.%). Slightly elevated TOC (0.74-0.99 wt.%) and sulphur contents (1.0-2.5 wt.%) occur in carbonate-free and jarosite-bearing ("Maikop-type") sediments directly below the paper shales (616-622 m). HI values are generally low (avg. 47 mgHC/gTOC) and are only slightly higher (max. 97 mgHC/gTOC) in the "Maikop-type" sediments.

The paper shales are rich in organic matter (avg. TOC: 4.35 wt.%; max. 13.27 wt.%) with very high HI values (avg. 456 mgHC/gTOC; max. 770 mgHC/gTOC). The very high TOC and moderately high sulphur contents (avg. 0.96 wt.%) result in high TOC/S ratios (avg. 5.14). Sediments above the paper shale contain low amounts of organic matter (avg. TOC: 0.64 wt.%) with low HI values (avg. 74 mgHC/gTOC). Both TOC and HI values show a general decreasing trend upwards in the section. Low sulphur contents (avg. 0.22 wt.%) result in moderately high TOC/S ratios (2.94). The average T_{max} value of the Diatom Formation is 422°C. PI values strongly depend on organic matter richness, and range from 0.01 to 0.10 for samples with S1 peaks ≤0.02 mgHC/g rock.

Organic petrography
Organic petrological investigations have been performed on four Paleocene samples with relatively
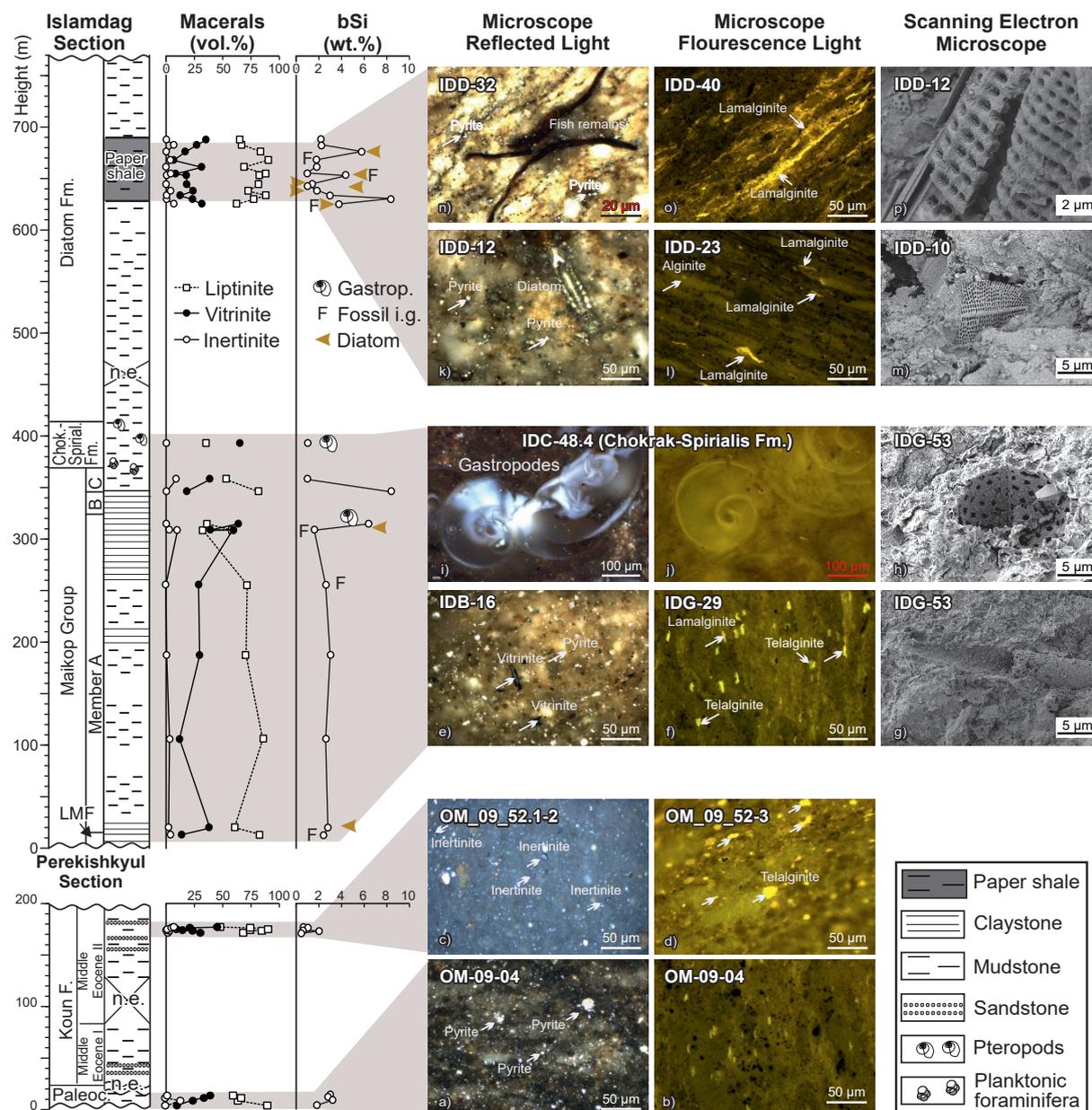
Fig. 8. Maceral percentages, percentages of biogenic silica (bSi), sample photomicrographs (left: white light; middle: fluorescence illumination), and (right) scanning electron microscope images of diatoms. Fossils i.g. comprise shell fragments and fish remains. (a,b) Paleocene; (c,d) Middle Eocene II; (e-h) Maikop Group; (i,j) Chokrak-Spirialis Formation; (k-p) Diatom Formation.

low TOC contents (1.0-1.1 wt.%), six samples from the Middle Eocene II (2.0-9.0 wt.% TOC), ten samples from the Maikop Group (1.6-5.8 wt.% TOC), a single sample from the Chokrak-Spirialis Formation (2.6 wt.% TOC), and 12 paper shale samples from the Diatom Formation (1.3-8.2 wt.% TOC).

The Paleocene samples contain large amounts of alginite (59-90 vol.%) dominated by lamalginite. Considerable amounts of telalginite (Fig. 8b) are found in the upper two samples. The percentage of vitrinite macerals increases upwards from 10 to 39 vol.%. Inertinite macerals occur in significant amounts in a single sample. The lowermost sample (OM-09-04) contains a considerable amount of pyrite (Fig. 8a).

The organic matter in the Middle Eocene II sediments is dominated by telalginite (38 vol.%) and lamalginite (31 vol.%), which occur in similar amounts (Fig. 8d). The terrigenous macerals vitrinite (avg. 24 vol.%) and inertinite (Fig. 8c; avg. 3 vol.%) are observed in minor amounts.

The maceral composition of the samples from the Maikop Group is dominated by liptinite (Fig. 8f). Lamalginite is generally more abundant than telalginite, but telalginite dominates in some samples from the lower part of the Maikop succession. Inertinite occurs in small percentages (≤10 vol.%). Vitrinite is the main maceral group in samples IDB-09 (309.95 m) and IDB-16 (316.4 m; Fig. 8e).

The sample from the Chokrak-Spirialis Formation (IDC-48.2) contains abundant gastropods (*Limacina* sp.) which are responsible for the high carbonate content of this sample (Fig. 8i,j). Vitrinite (65 vol.%) is significantly more abundant than liptinite (35 vol.%). Telalginite is the dominant liptinite maceral (30 vol.%).

Paper shales from the Diatom Formation contain large amounts of alginite (avg. 77 vol.%; Fig. 8l,o). The vitrinite percentage is on average 21 vol.%. Inertinite macerals are typically rare (max. 7 vol.%). With the exception of two samples from the base of the paper shale, lamalginite is more abundant than telalginite. Diatoms and fish remains are observed in many samples (Fig. 8k,m-p).

Vitrinite reflectance was determined for two samples from the Perekishkyul section (Middle Eocene II), five samples from the Maikop Group in the Islamdag section, and two samples from the Diatom Formation. All reflectance values are below 0.3 %R_o.

Biogenic silica

Diatoms were observed in samples from throughout the section. Therefore, a technique proposed by Zolitschka (1988) was applied to determine biogenic silica contents. The determined concentrations are generally low, but concentrations up to 10 wt.% were detected in samples below and above member B of the Upper Maikop Formation and in some paper shales within the Diatom Formation (Fig. 8). However, in some samples with microscopically visible diatom remains, biogenic silica contents are low.

Molecular composition of hydrocarbons

Biomarker data have been determined for 30 samples with high organic matter (OM) contents (Table 3). Characteristic chromatograms are shown in Fig. 9, and stratigraphic plots of selected biomarker ratios in Fig. 10. The significance of the biomarker parameters determined is summarised in Table 4. Facies- and maturity-related parameters are presented separately for the most relevant organic-rich intervals.

Middle Eocene II (Perekishkyul)

Six samples with high TOC contents (2.0-9.0 wt.%) from the upper part of the Perekishkyul section (Middle Eocene II) were investigated. These samples yielded relatively small amounts of extract (average 18 mg/gTOC). The *n*-alkane distributions of all of the samples show a predominance of long-chain *n*-alkanes (*n*-C_{26-31}) with an average value of 47 %, whereas mid-chain (23 %) and short-chain *n*-alkanes occur in significant lower amounts (12 %). CPI values range from 2.2 to 3.3.

Pristane/phytane (Pr/Ph) ratios are very low (<0.4). C_{25} HBI (highly branched isoprenoid) alkanes, markers for diatoms (Volkman *et al*., 1994), occur in significant amounts (average 13.3 µg/gTOC) and reach

a maximum in the lower part of the succession (27.3 and µg/gTOC; see Fig. 9). C_{25} HBI thiophenes are also present, but in significant lower concentrations (max. 0.4 µg/gTOC). Pentamethylicosane (PMI; Fig. 9) is found in all samples in low concentrations (avg. 1.6 µg/gTOC).

Steranes (avg. 49.83 µg/gTOC), sterenes (avg. 24.88 µg/gTOC) and steradienes (avg. 19.78 µg/gTOC) occur in significant amounts. The presence of steradienes, a product of sterol dehydration, is evidence for a very low maturity of the samples. The sterane distributions are dominated by C_{27} steranes (avg. 49 %), which are generally more abundant than C_{29} (32 %) and C_{28} homologues (20 %). Particularly high percentages of C_{27} steranes are found in two samples from the lower part of the succession. Steroids (Σ steranes + sterenes + steradienes)/hopanoids (Σ hopanes+hopenes) ratios are uniformly high (2.25-5.57) and correlate positively with Pr/Ph ratios ($R^2 = 0.88$).

ααα20S steranes and αββ steranes are not present. Hence, sterane isomerization ratios are 0 for all samples. The average S/(S+R) and ββ/(ββ+αα) isomerization ratios of C_{31} hopanes are 0.22 and 0.72, respectively. Dibenzothiophenes were not detected. Diterpenoids occur in very low concentrations (avg. 1.7 µg/gTOC).

Maikop Group (Islamdag)

One sample from the Lower Maikop Formation (IDF-07), together with nine samples from member A and two samples from member C of the Upper Maikop Formation in the Islamdag section were analysed. Sample IDC-48.2 from the Chokrak-Spirialis Formation is also included in this section because it is similar to the samples from member C. The extract yield increases upwards from 14 to 155 mg/gTOC within the Maikop Group. A strong positive correlation ($R^2 = 0.72$) with relative asphaltene percentages shows that high extract yields are mainly caused by high amounts of asphaltenes. A positive correlation also exists in the Maikop Group between extract yields and PI values ($R^2=0.54$). A relatively high extract yield of 74 mg/gTOC characterizes the uppermost sample from member A (IDB-16; 316.35 m). The extract yield in the sample from the Chokrak-Spirialis Formation is 45 mg/gTOC.

n-Alkane distributions are characterized by high percentages of mid- (avg. 41 wt.%) and long-chain *n*-alkanes (avg. 31 wt.%). Short-chain *n*-alkanes occur in minor amounts (avg. 13 wt.%). Long-chain *n*-alkanes dominate over mid-chain *n*-alkanes in the lowermost and uppermost sample. CPI values vary significantly between 1.39 and 5.39.

In several samples, crocetane most likely co-elutes in low abundances with phytane (e.g. Greenwood and Summons, 2003; Birgel *et al*., 2006), as indicated
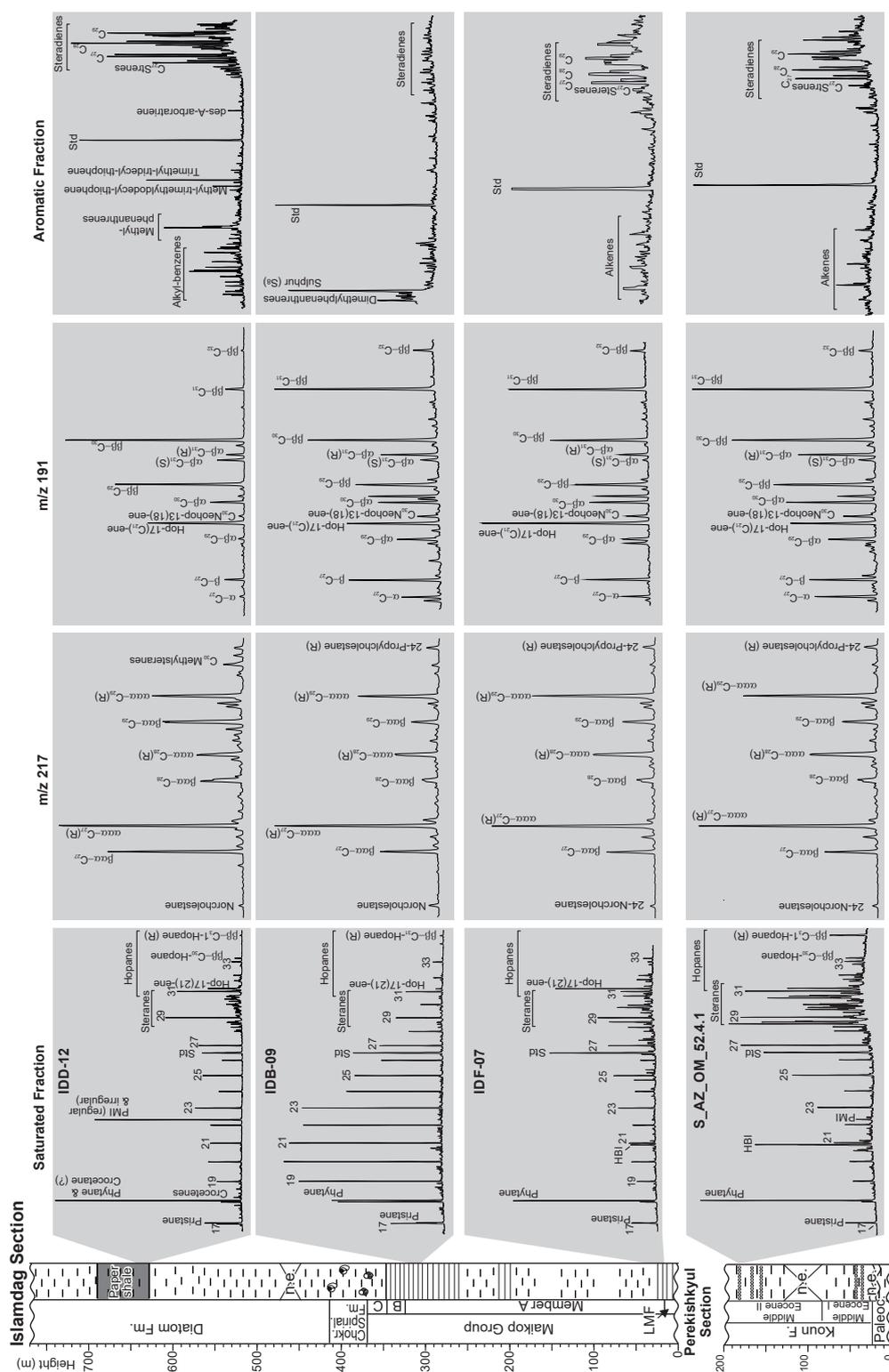
Fig. 9. Gas chromatograms and mass fragmentograms (*m/z* 217 and 191) of selected samples keyed to the stratigraphic column at the left.

by lower $\delta^{13}C$ values in comparison to pristane (see below). Consequently, Pr/Ph ratios cannot be determined reliably and the very low values recorded (avg. 0.19) should be considered with caution. C_{25} HBI-alkanes and C_{25} HBI-thiophenes occur in high amounts in the lower part of the section (e.g. IDF-39 [106.90 m], IDF-67 [188.30 m]). PMI (regular and irregular; Birgel *et al*., 2006) is present in several samples, reaching a

maximum concentration of 3.13 µg/gTOC at 316.35 m (IDB-16).

Steranes occur in all samples in high concentrations (avg. 68.33 µg/gTOC), and sterenes are present in most samples (avg. 4.32 µg/gTOC). The presence of steradienes is restricted to member A (avg. 4.33 µg/gTOC). Sterane distributions are dominated by C_{27} (avg. 40%) or C_{28} homologues. C_{29} steranes (avg.
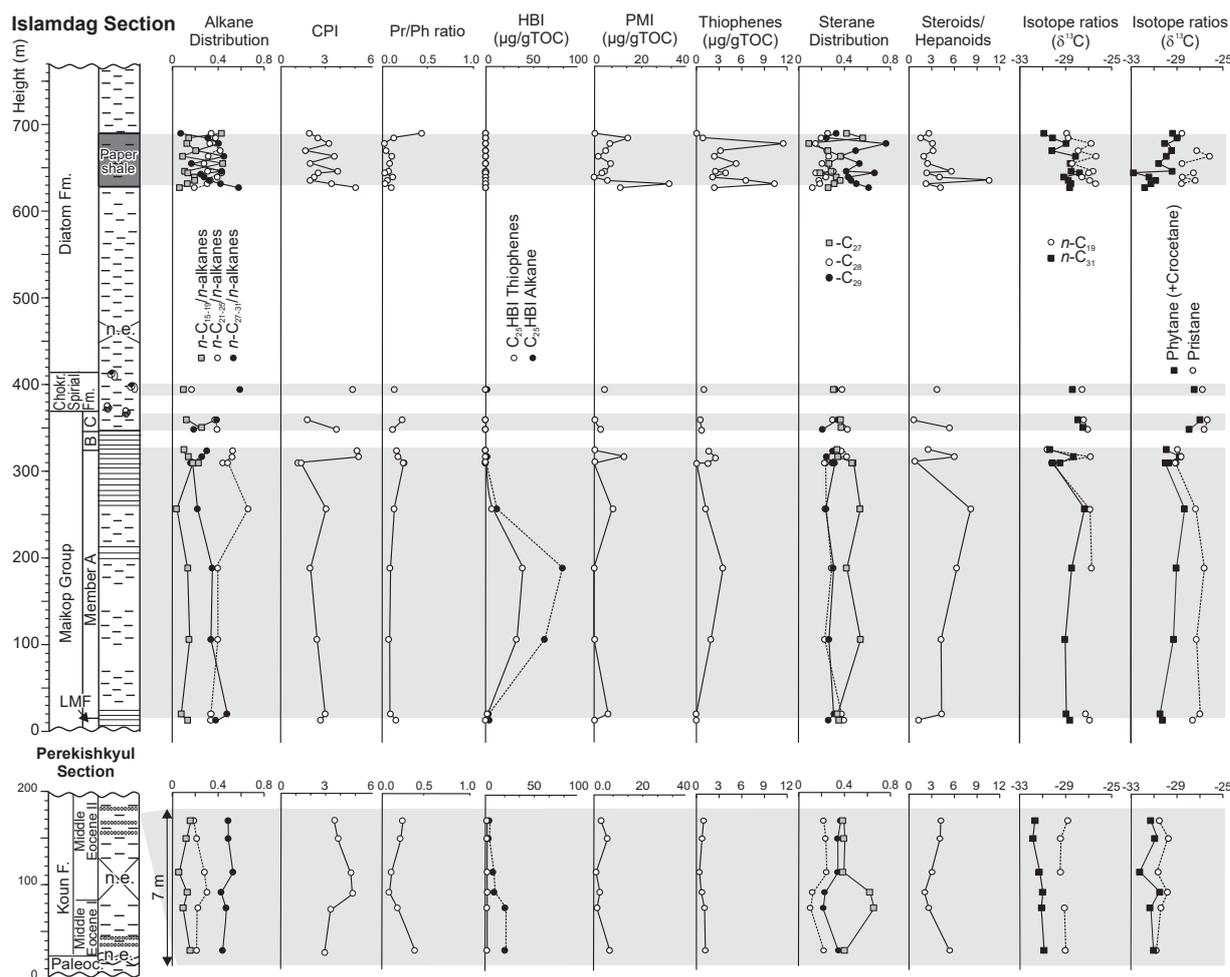
Fig. 10. Simplified lithological log of sediments exposed in the Perekishkyul and Islamdag sections and ratios of selected biomarkers and carbon isotope ratios of different molecules. Pa - Paleocene; Eoc. - Eocene; Fm. - Formation; CPI – Carbon Preference Index; HBI - highly branched isoprenoid; PMI – pentamethylicosane; TOC - total organic carbon; conc. ratios – concentration ratios.

28%) generally occur in low amounts. The steroids/ hopanoids ratio is generally very high (max. 8.23), but lower in a few samples from near the top of the Maikop Group.

Sterane isomerisation ratios are 0. The average S/ (S+R) and ββ/(ββ+αα)-C_{31} hopanes ratios are 0.27 and 0.71, respectively. Dibenzothiophene were detected in all samples, though in very low concentrations, and the maximum DBT/Phen ratio is only 0.17. C_{20} isoprenoid thiophenes, probably derived from phytane (e.g. Kutuzov *et al.*, 2020), have been detected (max.: 3.5 µg/gTOC) in most samples from the Upper Maikop Formation. Diterpenoids are also present in all samples, but with low concentrations (avg. 3.89 µg/gTOC). The maximum concentration (10.48 µg/gTOC) is observed at 106.90 m in sample IDF-39.

Diatom Formation (paper shale; Islamdag)
The Diatom Formation is represented by ten samples from the paper shale interval, as well as one underlying and one overlying sample. All samples yield considerable amounts of extract (avg. 47.5 mg/

gTOC). The maximum value (109.4 mg/gTOC) was observed in the low TOC sample (1.23 wt.%) above the paper shale (IDD-52). *n*-Alkane distributions are characterized by strongly varying percentages of short- (avg. 19 wt.%), mid- (avg. 34 wt.%) and long-chain *n*-alkanes (avg. 32 wt.%). CPI values are 1.92–5.18 and correlate well with the relative amount of long-chain *n*-alkanes ($R^2 = 0.83$).

Pr/Ph ratios could not be determined reliably because the phytane peak is most likely overlain by minor amounts of co-eluting crocetane. This is indicated by mass spectra and by differences in the C-isotope compositions of the isoprenoids (see below: e.g. Birgel *et al.*, 2006). It is further evidenced by the presence of crocetenes in low abundances (c.f. Elvert *et al.*, 2000). Based on mass spectra and $\delta^{13}C$ values, the C_{25} isoprenoid (PMI; avg. 9.41 µg/ gTOC) includes a contribution of irregular PMI which usually accompanies crocetane (Birgel *et al.*, 2006). Highly branched isoprenoid (HBI) alkanes are absent in the samples. C_{20} isoprenoid thiophenes (methyl-trimethyldodecyl-thiophene and trimethyl-tridecyl-

Table 3. Concentrations and concentration ratios of compounds and compound groups within the hydrocarbon fractions of Eocene, Oligocene and Miocene sediments from the Perekishkyul and Islamdag sections. EOM: extractable organic matter.

Sample	Depth (m)	TOC (wt.%)	HI (mg HC/g TOC)	PI S1/(S1+S2)	EOM (mg/g TOC)	Sat. HC	Arom. HC (wt.%, EOM)	NSO	Asphaltenes	n-C15-19/ n-Alkanes	n-C21-25/ n-Alkanes	n-C27-31/ n-Alkanes	CPI	Pr/Ph Crocetane?	C25 HBI Alkane (µg/gTOC)	C25 HBI Thioph.	PMI	C20 Isoprenoid Thiophenes
Diatom Formation																		
IDD-52	690.05	1.23	154	0.03	109.35	17.5	6.4	54	22	0.43	0.34	0.07	2.17	0.47	0.00	0.00	0.00	0.00
IDD-49	684.85	3.13	414	0.02	34.72	10.9	2.8	57	29	0.14	0.38	0.31	2.71	0.17	0.00	0.00	16.14	0.90
IDD-45	678.35	1.32	245	0.03	52.76	6.8	2.9	36	54	0.13	0.33	0.40	3.43	0.07	0.00	0.00	7.15	11.46
IDD-40	670.10	5.62	692	0.02	26.37	7.5	1.7	84	7	0.20	0.42	0.21	1.92	0.09	0.00	0.00	5.75	3.11
IDD-37	663.35	3.29	436	0.01	42.21	4.2	2.3	62	31	0.09	0.31	0.45	3.78	0.15	0.00	0.00	2.27	2.31
IDD-31	655.25	9.33	633	0.03	35.95	4.4	1.4	81	14	0.44	0.28	0.17	2.22	0.13	0.00	0.00	8.01	5.24
IDD-23	646.45	2.90	422	0.01	45.64	5.4	3.6	65	26	0.11	0.31	0.43	3.99	0.12	0.00	0.00	5.11	2.47
IDD-21	644.75	10.76	643	0.04	76.84	2.1	1.1	55	41	0.13	0.43	0.28	2.74	0.08	0.00	0.00	4.31	3.87
IDD-17	640.05	5.89	624	0.02	25.35	6.7	2.8	78	13	0.19	0.39	0.25	2.48	0.16	0.00	0.00	0.00	2.18
IDD-14	635.65	6.61	696	0.03	39.72	4.2	2.1	61	33	0.19	0.33	0.32	2.22	0.10	0.00	0.00	5.98	6.52
IDD-12	627.40	8.20	617	0.02	34.33	4.3	1.6	74	21	0.13	0.30	0.42	3.60	0.08	0.00	0.00	36.12	2.40
IDD-10	631.90	1.33	206	0.03	46.69	9.6	7.1	55	29	0.07	0.22	0.58	5.18	0.15	0.00	0.00	12.70	10.31
Chokrak-Spirialis Formation																		
IDC-48.2	394.35	2.37	214	0.06	44.66	2.3	0.6	34	63	0.09	0.16	0.57	5.10	0.18	1.79	0.00	1.04	0.97
Maikop Group (Lower and Upper Maikop Fm.)																		
IDB-67	359.65	5.72	491	0.08	154.35	2.3	0.2	22	76	0.10	0.37	0.38	2.03	0.26	0.00	0.00	0.00	0.49
IDB-53	347.55	3.79	240	0.06	80.10	1.1	0.1	37	61	0.25	0.39	0.18	3.91	0.16	0.00	0.00	1.43	0.64
IDB-23	323.65	3.08	252	0.04	47.52	9.3	1.5	48	41	0.08	0.52	0.30	5.28	0.20	0.00	0.00	0.00	1.66
IDB-16	316.35	1.95	123	0.08	73.80	12.0	2.6	54	31	0.12	0.53	0.24	5.39	0.20	1.94	0.00	3.14	2.54
IDB-09	309.95	4.49	140	0.04	42.38	22.0	2.6	40	36	0.22	0.44	0.15	1.39	0.28	0.00	0.00	0.00	1.58
IDG-53	310.25	1.64	49	0.08	45.63	7.1	1.3	41	50	0.17	0.48	0.17	1.55	0.27	0.00	0.00	0.00	0.00
IDG-29	256.85	4.23	205	0.04	34.30	13.1	2.2	56	29	0.03	0.67	0.21	3.24	0.16	5.55	6.97	1.98	1.21
IDF-67	188.30	2.25	238	0.04	39.00	24.3	3.9	56	16	0.12	0.38	0.34	2.26	0.12	43.99	40.49	0.00	3.46
IDF-39	106.90	4.10	311	0.03	23.34	14.4	3.8	66	16	0.14	0.39	0.33	2.61	0.11	30.75	33.98	0.00	1.91
IDF-10	20.40	2.95	264	0.02	19.99	18.0	3.7	61	17	0.06	0.32	0.47	3.31	0.11	1.37	1.96	1.46	0.00
IDF-07	13.20	2.23	42	0.03	14.21	16.6	8.5	50	25	0.12	0.34	0.37	3.02	0.18	4.12	0.00	0.00	0.00
Koun Formation (Middle Eocene II)																		
09_52_7-2	177.40	8.99	385	0.02	22.21	14.1	3.6	67	15	0.15	0.19	0.48	2.57	0.29	3.39	0.25	1.66	0.93
09-52_6-1	176.60	8.58	352	0.02	19.54	13.9	4.8	67	14	0.12	0.21	0.48	2.71	0.27	2.34	0.35	1.84	0.77
09_52_4-1	175.10	2.00	171	0.02	17.10	6.9	4.3	68	20	0.05	0.28	0.52	3.20	0.21	9.29	0.19	1.19	0.39
09_52_3	174.20	3.27	371	0.01	16.02	9.8	4.7	73	12	0.12	0.30	0.42	3.26	0.19	10.78	0.38	1.51	0.67
09_52_2-2	173.50	5.42	326	0.02	17.45	13.8	4.5	71	11	0.09	0.20	0.46	2.43	0.25	27.29	0.34	1.32	1.04
09_52_1-2	171.60	7.19	371	0.02	18.30	12.8	3.9	59	25	0.15	0.21	0.43	2.20	0.38	27.06	0.36	2.19	1.18

Islamdag section — Perekishkyul Section

Table 3, continued.

Sample	Depth (m)	Steranes (µg/gTOC)	C27 Steranes/ Steranes	C28 Steranes/ Steranes	C29 Steranes/ Steranes	Sterenes (µg/gTOC)	Steradienes (µg/g TOC)	Hopanes (µg/gTOC)	S/(S+R) C31 Hopanes	ββ/(ββ+αβ) C31 Hopanes	Hopenes (µg/gTOC)	Steroids/ Hopanoids	DBT/ Phen	Diterpenoids (Arom.) (µg/gTOC)	Monoarom. Steroids (µg/gTOC)
Diatom Formation															
IDD-52	690.05	9.30	0.33	0.25	0.42	1.27	10.48	7.64	0.47	0.49		2.76	0.73		
IDD-49	684.85	17.12	0.24	0.20	0.56	1.58	4.37	8.31	0.41	0.70	4.59	1.79		0.58	
IDD-45	678.35	5.42	0.76	0.15	0.09	7.25	83.40	8.39	0.42	0.65	21.08	3.26		2.32	
IDD-40	670.10	2.41	0.50	0.25	0.26	1.89	8.69	2.38	0.48	0.71	1.50	3.34		0.76	
IDD-37	663.35	7.56	0.37	0.26	0.37	4.70	31.13	4.95	0.45	0.60	15.34	2.14		8.78	
IDD-31	655.25	10.29	0.53	0.20	0.27	7.06	22.52	4.37	0.43	0.57	11.23	2.56		1.35	
IDD-23	646.45	5.62	0.42	0.30	0.28	8.45	159.35	5.60	0.41	0.66	24.79	5.71		2.03	
IDD-21	644.75	6.72	0.66	0.15	0.19	8.97	48.28	4.94	0.40	0.70	21.60	2.41		2.19	
IDD-17	640.05	6.44	0.43	0.24	0.33	3.41	20.05	5.01	0.41	0.69	2.27	4.11		1.58	
IDD-14	635.65	19.16	0.46	0.18	0.36	18.41	98.72	3.21	0.35	0.54	9.48	10.75		2.18	
IDD-12	627.40	13.07	0.50	0.18	0.31	5.13	22.65	8.03	0.41	0.49	8.79	2.43		0.56	
IDD-10	631.90	44.21	0.56	0.12	0.31	5.47	174.67	26.61	0.33	0.76	25.19	4.33		3.57	
Chokrak-Spirialis Formation															
IDC-48.2	394.35	64.60	0.31	0.37	0.32	0.55	0.00	17.33	0.32	0.71		3.76	0.05	2.45	
Maikop Group (Lower and Upper Maikop Fm.)															
IDB-67	359.65	44.27	0.37	0.29	0.34	0.59	0.00	50.08	0.21	0.69	5.70	0.80	0.06	1.64	
IDB-53	347.55	73.30	0.37	0.42	0.21	0.44	0.00	12.23	0.28	0.72	1.18	5.50	0.05	0.77	
IDB-23	323.65	82.18	0.34	0.37	0.29	1.34	2.78	24.94	0.31	0.90	8.48	2.58	0.09	4.24	0.75
IDB-16	316.35	112.74	0.34	0.42	0.24	0.00	3.74	10.14	0.39	0.74	9.05	6.07	0.10	6.41	2.04
IDB-09	309.95	15.33	0.48	0.23	0.29	5.86	6.94	8.60	0.28	0.73	23.89	0.87	0.07	4.09	2.55
IDG-53	310.25	10.46	0.47	0.22	0.31	0.82	1.04	11.06	0.25	0.70	5.22	0.76	0.05	1.38	0.28
IDG-29	256.85	82.39	0.53	0.23	0.24	5.85	5.39	5.98	0.15	0.60	5.39	8.23	0.16	2.45	0.44
IDF-67	188.30	166.70	0.42	0.28	0.30	10.87	11.04	12.76	0.23	0.59	16.82	6.38	0.17	4.89	1.48
IDF-39	106.90	47.78	0.54	0.22	0.24	12.82	15.63	6.49	0.29	0.71	11.39	4.26	0.10	10.48	1.80
IDF-10	20.40	85.89	0.34	0.37	0.29	8.86	5.46	9.76	0.23	0.65	12.97	4.41	0.10	0.62	1.59
IDF-07	13.20	34.28	0.35	0.39	0.26	3.82	0.00	10.06	0.26	0.82	16.60	1.43	0.06	7.30	1.15
Koun Formation (Middle Eocene II)															
09_52_7-2	177.40	75.12	0.40	0.23	0.38	27.03	23.58	19.10	0.29	0.84	9.69	4.37		2.36	0.50
09-52_6-1	176.60	63.38	0.41	0.24	0.35	29.30	24.56	18.97	0.25	0.84	8.37	4.29		2.15	0.49
09_52_4-1	175.10	43.65	0.40	0.25	0.35	16.48	10.13	16.37	0.19	0.69	6.13	3.12		1.22	0.31
09_52_3	174.20	17.70	0.63	0.13	0.24	21.21	13.96	14.81	0.13	0.67	8.71	2.25		1.27	0.38
09_52_2-2	173.50	29.45	0.67	0.11	0.22	24.26	17.71	13.81	0.23	0.66	11.52	2.82		1.70	0.51
09_52_1-2	171.60	69.66	0.41	0.23	0.36	30.99	29.28	13.00	0.22	0.77	10.32	5.57		1.55	0.49

Table 4. Application and significance of biomarker proxies (details in Peters et al., 2005 and references therein).

Biomarker proxy	Application	Significance
n-Alkane distribution	Source	*n*-C_{15-19} Algae, Bacteria; *n*-C_{21-25} Algae, Bacteria, Macrophytes; *n*-C_{27-31} Vascular plants
Carbon Preference Index (CPI)	Source, Maturity	CPI > 1.0 of long-chain alkanes (> *n*-C_{23}) Land plants, Low maturity
Pristane/Phytane (Pr/Ph)	Environment, Source	Pr/Ph < 1.0 Reducing; Pr/Ph > 3.0 Oxidizing, Land plants
Crocetane, PMI (irregular)	Source, Environment	Archaea (methanogenic and methanothrophic); Water column stratification
C_{25} HBI alkane, thiophenes	Source	Diatoms (marine)
Thiophenes (DBT, isoprenoid)	Environment	Water column stratification (marine)
24-Norcholestane	Source, Age	Diatoms, Cretaceous or younger
C_{27} Steranes/Steranes	Source	Phytoplankton, Zooplankton
C_{28} Steranes/Steranes	Source, Age	Algae (Diatoms); C_{28}/C_{29} > 1.0 Cretaceous or younger
C_{29} Steranes/Steranes	Source	Plants (+ specific algae)
C_{30} Steranes	Source	Marine algae
Steroids	Source	Eukaryotes
Hopanoids	Source	Prokaryotes (Bacteria)
S/(S+R) C_{31} Hopanes	Maturity	Equilibrium of 0.60 top of oil window
$\beta\beta/(\beta\beta + \alpha\beta)$ C_{31} Hopanes	Maturity, Environment	Decreasing with increase in maturity; pH in peat
Diterpenoids	Source	Land plants (Gymnosperms)

thiophene; Fig. 9) occur in significant amounts (max. 11.5 µg/gTOC).

Steradienes are present in high abundance within the aromatic hydrocarbon fractions (avg. 57.03 µg/gTOC) and are significantly more abundant than steranes (avg. 12.28 µg/gTOC) and sterenes (6.13 µg/gTOC). Sterane distributions are dominated by C_{27} steranes (avg. 48%). C_{29} steranes (avg. 31%) occur only in the two uppermost samples, whereas C_{28} steranes occur in small amounts (avg. 21%). However, steradienes contain high relative proportions of C_{28} homologues (Fig. 9). The steroids/hopanoids ratio is generally high (avg. 3.8) and reaches a maximum value (10.75; IDD-14) near the base of the succession.

Sterane isomerisation ratios are 0. The average S/(S+R) C_{31} hopanes ratio (0.41) is higher and the $\beta\beta/(\beta\beta+\alpha\alpha)$ ratio (0.63) is lower than in the underlying units. Dibenzothiophene was detected only in the uppermost sample (DBT/Phen: 0.73). Concentrations of diterpenoids are typically low (0.56-3.57 µg/gTOC), but are high in sample IDD-37 (8.78 µg/gTOC).

Compound-specific C isotope ratios

Isotope data for *n*-alkanes, as well as for pristane [$\delta^{13}C_{pristane}$] and phytane [$\delta^{13}C_{phytane}$] were determined on the 30 biomarker samples (Table 5). The $\delta^{13}C$ values for pristane were obtained by integrating the overlapping peaks of *n*-C_{17}, present in very low abundances, and pristane. $\delta^{13}C$-values of short- (*n*-C_{19}) and long-chain *n*-alkanes (*n*-C_{31}), as well as of pristane and phytane, are plotted versus depth in Fig. 10.

Isotope ratios of additional compounds (i.e. PMI [$\delta^{13}CPMI$], HBIs [$\delta^{13}CHBI$], Hop17(21)ene [$\delta^{13}CHop$], specific steranes and arborane) could be determined for some samples and are listed in Table 5.

n-C_{18} to *n*-C_{24} alkanes derived from Middle Eocene II sediments in the Perekishkyul section

are characterized by a decrease in $\delta^{13}C$ values with increasing chain length from -29.0 to -31.5 ‰. No further decrease could be observed for longer-chained *n*-alkanes (Fig. 11a). *n*-Alkanes in samples from the Maikop Group and the Chokrak-Spirialis Formation in the Islamdag section are generally isotopically heavier (Fig. 11b-d), although three isotopically light samples (IDG-53; IDB-09; IDB-23) occur near the top of member A (Fig. 11c). The paper shales in the Diatom Formation show varying isotope patterns (Fig. 11e-g) with strongly negative values in some samples from its upper part (Fig. 11g).

$\delta^{13}C_{pristane}$ and $\delta^{13}C_{phytane}$ values are similar (difference ≤1 ‰) in samples from the Perekishkyul section and several samples from the Islamdag section (Fig. 11h). This suggests a common precursor (i.e. chlorophyll). In contrast, phytane is significantly enriched in ^{12}C in the lowermost four Maikop Group samples from Islamdag and seven samples from the Diatom Formation, suggesting co-elution of phytane with isotopically-light crocetane, an irregular C_{20}-isoprenoid (Thiel *et al*., 1999).

$\delta^{13}CHBI$ values in middle Eocene sediments range from -31.1 to -29.7 ‰ and are less negative in the Maikopian sediments (-29.6 to -28.5 ‰). The range of $\delta^{13}CPMI$ values was also determined on some samples from the Diatom Formation, and yielded even more negative values (-34.2 to -36.5 ‰).

DISCUSSION

Thermal maturity and its influence on biomarker ratios

Many geochemical parameters used for the reconstruction of depositional environment and the assessment of source rock potential are influenced by the thermal maturity of the rocks. Hence the
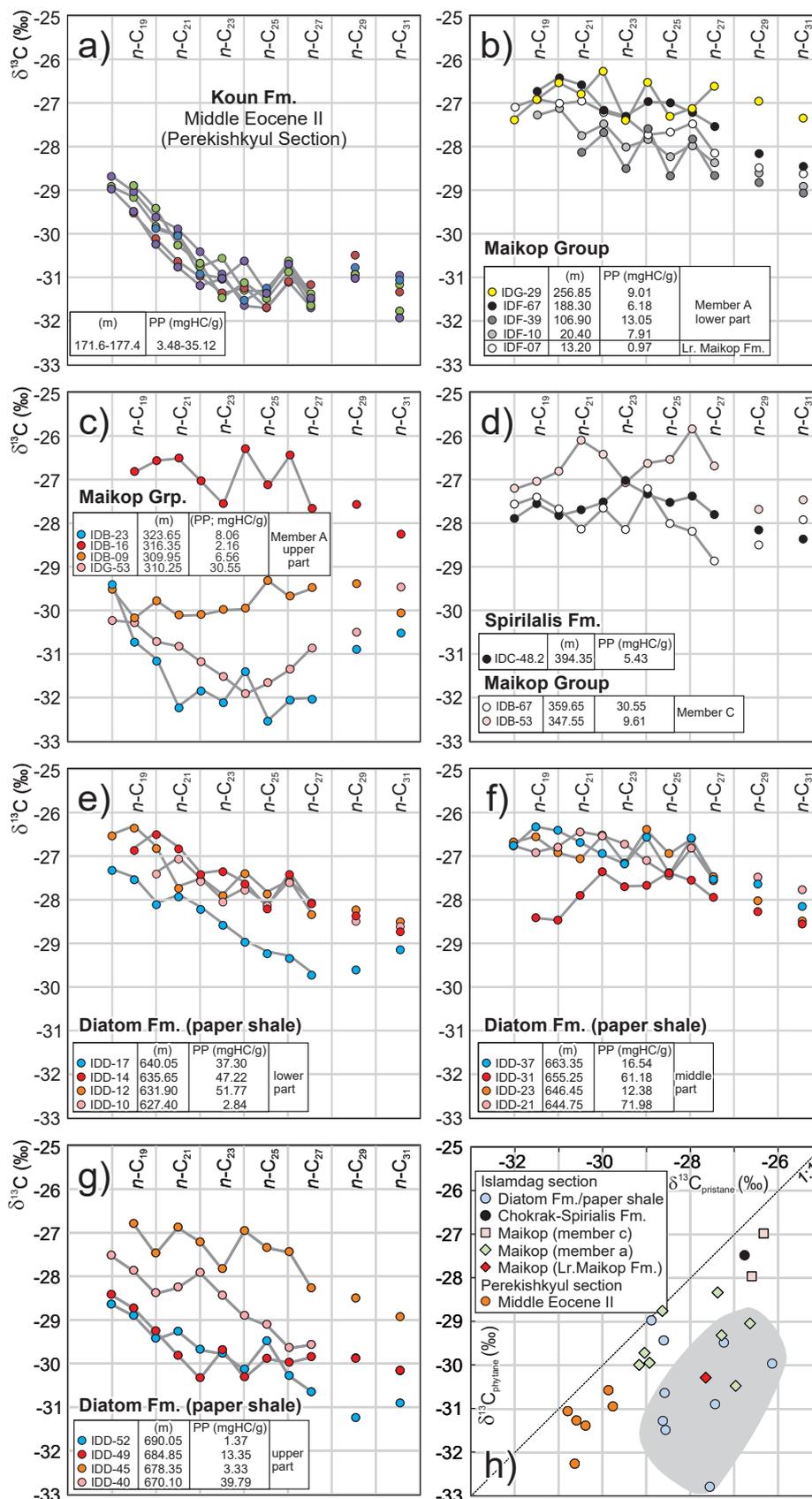
Fig. 11. Carbon isotope ratios (δ^{13}C) of *n*-alkanes in samples from: (a) the Koun Formation (Middle Eocene II) in the Perekishkyul section; (b) the Lower Maikop Formation and Maikop member A; (c) the Maikop member A; (d) the Maikop member C and the Chokrak-Spirialis Formation; (e-g) the Diatom Formation. (h) cross-plot of δ^{13}C values of pristane (δ^{13}C$_{pristane}$) versus phytane (δ^{13}C$_{phytane}$). Grey field indicates samples with lower δ^{13}C$_{phytane}$ values compared to pristane which may indicate an effect due to the co-elution of isotopically light crocetane.

Table 5. Compound specific carbon isotope (δ13C, ‰ V-PDB) of Eocene, Oligocene and Miocene sediments from the Perekishkyul and Islamdag sections.

Section	Sample	n-C18	n-C19	nC20	n-C21	n-C22	n-C23	n-C24	n-C25	n-C26	n-C27	n-C29	n-C31	Pristane (+n-C17)	Phytane (+Crocetane?)	PMI	C25 HBI	Hop17(21)ene	Arborene	Steranes ααα-C27(R)	ααα-C28(R)	ααα-C29(R)
Diatom Formation																						
Islamdag section	IDD-52	-28.6	-28.9	-29.4	-29.3	-29.7	-29.76	-30.1	-29.5	-30.3	-30.6	-31.23	-30.9	-28.60	-29.43							
	IDD-49	-28.4	-28.7	-29.3	-29.8	-30.3	-29.68	-30.3	-29.9	-30.0	-29.8	-29.88	-30.2	-28.88	-28.97							
	IDD-45		-26.8	-27.5	-26.9	-27.2	-27.83	-27.0	-27.4	-27.4	-28.3	-28.5	-28.9		-30.06			-29.5				
	IDD-40	-27.5	-27.9	-28.4	-28.3	-27.9	-28.44	-28.9	-29.1	-29.6	-29.6	-29.87	-30.2	-27.23	-29.48							
	IDD-37	-26.8	-26.3	-26.4	-26.7	-27.0	-27.19	-26.6	-27.4	-26.6	-27.5	-27.65	-28.2	-26.13	-29.96	-35.4		-31.6				
	IDD-31		-28.4	-28.5	-27.9	-27.4	-27.71	-27.7	-27.4	-27.6	-28.0	-28.28	-28.6	-28.58	-30.63			-32.9				
	IDD-23	-26.7	-26.6	-26.9	-27.1	-26.5	-27.17	-26.4	-27.0	-26.6	-27.5	-28.03	-28.5	-27.55	-29.41			-30.8				
	IDD-21	-26.8	-26.9	-26.8	-26.5	-26.6	-26.74	-27.1	-27.5	-26.8	-27.6	-27.49	-27.8	-28.56	-32.78			-32.9				
	IDD-17	-27.3	-27.6	-28.1	-27.9	-28.2	-28.59	-29.0	-29.2	-29.4	-29.7	-29.61	-29.2	-27.43	-31.48							
	IDD-14		-26.9	-26.5	-26.9	-27.4	-27.37	-27.7	-28.2	-27.4	-28.1	-28.38	-28.7	-28.62	-30.89			-31.2				
	IDD-12	-26.6	-26.4	-26.8	-27.8	-27.6	-27.92	-27.4	-27.9	-27.6	-28.4	-28.24	-28.5		-31.27	-36.5		-31.8				
	IDD-10			-27.4	-27.1	-27.6	-28.06	-27.8	-28.1	-27.6	-28.1	-28.5	-28.6		-31.79	-34.2		-30.2	-24.9			
Chokrak-Spirialis Fm.																						
	IDC-48.2	-27.9	-27.6	-27.8	-27.7	-27.5	-27.03	-27.3	-27.5	-27.4	-27.8	-28.16	-28.4	-26.76	-27.48		-26.2	-30.3		-26.4	-27.1	
Maikop Group (Lower and Upper Maikop Fm.)																						
	IDB-67	-27.6	-27.4	-27.7	-28.1	-27.7	-28.15	-27.2	-28.0	-28.2	-28.9	-28.5	-27.9	-26.32	-26.98					-26.8		
	IDB-53	-27.2	-27.1	-26.8	-26.1	-26.4	-27.08	-26.6	-26.6	-25.9	-26.7	-27.69	-27.5	-26.59	-27.96					-27.4	-27.1	
	IDB-23	-29.3	-30.6	-31.0	-32.1	-31.7	-31.97	-31.3	-32.4	-31.9	-31.9	-30.75	-30.4	-28.92	-29.94					-28.8	-28.8	-29.1
	IDB-16		-26.8	-26.6	-26.5	-27.0	-27.56	-26.3	-27.1	-26.5	-27.7	-27.58	-28.3	-28.63	-28.75			-29.7		-27.5	-27.7	-28.4
	IDB-09	-29.5	-30.2	-29.8	-30.1	-30.1	-29.98	-30.0	-29.3	-29.7	-29.5	-29.39	-30.1	-29.04	-29.71							
	IDG-53	-30.2	-30.3	-30.7	-30.8	-31.2	-31.51	-31.9	-31.7	-31.3	-30.9	-30.5	-29.5	-29.16	-29.99							
	IDG-29	-27.4	-26.9	-26.5	-26.8	-26.3	-27.39	-26.5	-27.3	-27.1	-26.6	-26.95	-27.3	-27.37	-28.33		-25.6	-30.0		-27.2	-27.4	-26.8
	IDF-67		-26.8	-26.4	-26.6	-27.2	-27.32	-27.0	-27.0	-27.2	-27.6	-28.17	-28.4	-26.63	-29.04		-25.9	-29.6		-27.2	-26.7	-27.1
	IDF-39				-28.1	-27.7	-28.51	-27.6	-28.7	-27.8	-28.7	-28.83	-29.1	-27.28	-29.31		-27.1	-29.8				
	IDF-10		-27.3	-27.1	-27.8	-27.5	-28.02	-27.9	-28.2	-28.0	-28.4	-28.61	-28.9	-26.96	-30.47			-30.8				
	IDF-07	-27.1	-26.9	-27.0	-27.0	-27.2	-27.35	-27.7	-27.7	-27.5	-28.2	-28.49	-28.6	-27.64	-30.28		-26.5	-32.2		-28.2		
Koun Formation (Middle Eocene II)																						
Perekishkyul section	09_52_7-2		-28.9	-29.4	-30.3	-30.7	-31.46	-31.1	-31.5	-30.9	-31.6	-30.93	-31.8	-30.59	-31.26			-32.6		-29.9		
	09_52_6-1	-29.0	-29.5	-30.2	-30.8	-31.2	-31.02	-30.6	-31.4	-30.7	-31.5	-31.02	-31.9	-29.76	-30.94			-33.8		-29.8	-30.1	
	09_52_4-1		-29.5	-30.1	-30.6	-31.0	-31.35	-31.2	-31.7	-31.1	-31.2	-30.49	-31.3	-30.63	-32.25		-31.1	-34.0		-30.2	-30.1	-29.8
	09_52_3			-29.9	-30.1	-30.9	-31.04	-31.5	-31.2	-30.7	-31.5	-30.77	-31.1	-29.86	-30.57		-30.9	-32.9		-29.4		-29.5
	09_52_2-2	-28.9	-29.2	-29.8	-30.0	-30.7	-30.56	-31.3	-31.3	-30.6	-31.4	-30.97	-31.2	-30.383	-31.38		-29.7	-32.5		-30.2	-30.6	-30.7
	09_52_1-2	-28.7	-29.0	-29.6	-29.9	-30.4	-30.92	-31.6	-31.7	-31.1	-31.7	-30.92	-31.0	-30.79	-31.05		-30.4	-32.0		-29.2	-29.4	-29.9

thermal overprint is discussed first, and depositional environment and hydrocarbon potential are then considered in the following sections.

The low vitrinite reflectance values (<0.3 %R$_r$) and the low average T$_{max}$ values obtained for samples from all of the studied sedimentary units (405-424°C; Table 2) are evidence of very low maturity. The low maturity is also supported by other geochemical parameters, such as high CPI values, high concentrations of sterenes and steradienes, the absence of $\alpha\alpha\alpha$ steranes with an S configuration, and the absence of $\alpha\beta\beta$ steranes. Isomerisation of C$_{31}$ hopanes is low in samples from the Perekishkyul section and in the Maikop Group samples from the Islamdag section, but significantly higher in samples from the Diatom Formation. This upward increase in isomerisation ratios is a facies effect rather than a maturity effect. Similarly, higher isomerisation ratios are observed in Jurassic rocks containing kerogen Type I than in rocks with kerogen Type II (Neumeister *et al.*, 2015).

Classical maturity parameters such as vitrinite reflectance, T$_{max}$ values and hopane isomerisation ratios do not show an increase with the age (and the burial depth) of the sediments. However, the fact that monoaromatic steroids occur (in very low concentrations) exclusively in Eocene sediments and in the Maikop Group, and that steradiene concentrations are higher than sterane concentrations only in the Diatom Formation, may reflect a subtle downward-increasing thermal overprint.The very low maturity may influence facies-dependent molecular proxies. For example, the incomplete reduction of steradienes and sterenes may be responsible for the lack of diasteranes and may also influence the relative sterane percentages. This is evidenced by differences in the relative abundances of C$_{27}$, C$_{28}$ and C$_{29}$ homologues of steradienes and steranes, respectively, in samples from the Diatom Formation (Fig. 9). Moreover, the observed low concentrations of DBT and the resulting very low DBT/Phen ratios (Table 3) may be due to the very low maturity rather than the limited availability of free H$_2$S (e.g. Hughes *et al.*, 1995).

This interpretation is supported by the high concentration of other sulphur-containing compounds (e.g. isoprenoid thiophenes in the Diatom Formation; HBI thiophenes in the Eocene and Maikop Group samples). The sample overlying the paper shale (IDD-52) is the only sample with a high DBT/Phen ratio (0.73). Moreover, Pr/Ph ratios may be influenced by the low maturity of the samples as phytane is released preferentially during early diagenesis (Volkman and Maxwell, 1986; Peters *et al.*, 2005). Pr/Ph ratios in the marginally mature Maikop Group at Lahich range from 1 to 3 (Bechtel *et al.*, 2014), whereas ratios in immature Maikop Group sediments at Angeheran were constantly below 1 (Bechtel *et al.*, 2013).

Depositional environment of organic-rich sediments

Middle Eocene II (Perekishkyul section)

Organic-rich layers with TOC contents between 2 and 12 wt.% are intercalated with low-TOC shaly sediments in the Perekishkyul section. These alternations were studied in detail between 171.5 m and 178.5 m (Figs 5, 10), but individual, unstudied, organic-rich layers were also observed between 135 m and 142 m, suggesting that they cover a much greater stratigraphic interval than that currently sampled. Thus, it is difficult to estimate the cumulative thickness of the organic -rich layers, but they probably do not exceed 2 m at the studied location.

Maceral analysis shows that the organic matter is dominated by aquatic biomass but with a significant input of land plant material. In addition to the abundant vitrinite and inertinite macerals, the presence of the terrigenous organic matter fraction is indicated by high percentages of long-chain *n*-alkanes with a significant odd-even predominance. Land plant-derived biomarkers (diterpenoids) occur in small amounts with a slight upward-increasing trend. The dominance of diterpenoids suggests that vegetation was dominated by gymnosperms (e.g. Bechtel *et al.*, 2008). This is in agreement with the observation that gymnosperm pollen are notably more abundant than angiosperm pollen (Bati, 2015).

The aquatic biomass is represented by high percentages of lam- and telalginite, indicating contributions from both algal/bacterial mat material and planktonic algae. Very high C$_{27}$ sterane percentages also indicate a predominance of marine algal material. Although the percentage of biogenic silica determined with the technique proposed by Zolitschka (1998) was low (Fig. 8), significant concentrations of isotopically light (-30.5 ‰) HBIs indicate the high productivity of marine diatoms. This is further evidenced by elevated relative abundances of 24-methylcholesta-5,22-diene and 24-methylcholesta-5,24(28)-diene, derived from sterols found in high concentrations in the extracts of diatoms (Rampen *et al.*, 2010). The presence of the C$_{30}$ sterane 24-*n*-propyl-5α-cholestane (20R) indicates a marine depositional environment, as 24-*n*-propylcholestanes have as yet only been identified in marine Chrysophyte algae (Moldowan *et al.*, 1990).

δ^{13}C values of Pr and Ph (Fig. 11h) indicate their similar source (i.e. chlorophyll), and Pr/Ph ratios may therefore be used as a redox parameter (Didyk *et al.*, 1978). Even considering maturity effects (*see above*), the very low Pr/Ph ratios obtained are consistent with anoxic conditions. The observed depth trend suggests that the most oxygen-deficient conditions occurred during deposition of the middle part of the succession. The presence of PMIs, most likely including minor amounts of irregular PMI

characteristic of methanogenic and methanotrophic archaea (e.g. Schouten *et al*., 1997; Greenwood and Summons, 2003), also supports strictly anoxic conditions. The presence of isoprenoid and HBI thiophenes, although in generally low concentrations (0.83 and 0.31 µg/gTOC), confirms the availability of free H_2S during early diagenesis.

HI values of organic-rich sediments vary significantly (Table 2). However, S2 and TOC values correlate well ($R^2 = 0.99$; Fig. 7). The positive intercept and the slope of the regression line show significant retention of S2 hydrocarbons on the shale matrix (mineral matrix effect; Espitalié *et al*., 1984), and that all organic-rich samples contain a similar kerogen Type II with a true HI (*sensu* Langford and Blanc-Valleron, 1990) of 412 mgHC/gTOC. The homogeneity of the organic matter is also reflected by the similar isotope patterns of the *n*-alkanes (Fig. 11). A strong mineral matrix effect was also indicated by analyses of kerogen concentrates from interlayered low-TOC shaly rocks. Whereas whole rock samples had low HI values (avg. 59 mgHC/gTOC; Table 2), isolated kerogens yield HI values similar to those of organic-rich sediments (>400 mgHC/gTOC; Saint-Germès *et al*., 2002). This shows that despite the widely differing TOC contents, the type of organic matter is similar in organic-rich and organic-poor sediments. Hence, layers with high TOC contents may represent the background sediment, whereas low TOC contents may result from dilution by clastic material.

Maikop Group (Islamdag Section)
The exposed part of the Maikop Group in the Islamdag section is 364 m thick. Significant progress has been achieved in age-dating this unit, and the new Re/Os age from the base of member A (30.0 ± 1.0 Ma) shows that sediment deposition in the Islamdag section began during the late Solenovian (Fig. 2). The nominal Re/Os age determined near the top of member A is 17.2 ± 3.2 Ma (Washburn *et al*., 2019). The Tarkhanian flooding event, which resulted in the cessation of deposition of the Maikop Group, was recently dated as 14.85 Ma (Palcu *et al*., 2019b). Using these age constraints, remarkably low sedimentation rates (~25 m/Ma) can be determined for the Upper Maikop Formation. The low sedimentation rates agree with the palaeogeographic setting of the study area in the deepest part of the Eastern Paratethys (Popov *et al*., 2004; 2008).

The Maikop Group in the Islamdag section begins with a 16 m thick interval rich in *Botryococcus braunii* and *Batiacasphaera* sp. indicating deposition in a basin with reduced salinity. This interval represents low salinity conditions of the Paratethys-wide Solenovian Event (Zaporozhets and Akhmetiev, 2015). Therefore, this interval is attributed to the Lower Maikop Formation (*sensu* Weber, 1935). The early Solenovian

Event itself (early NP23), often characterized by carbonate-rich sediments (Polbian or Ostracoda Bed; Gavrilov *et al*., 2017; Sachsenhofer *et al*., 2017, 2018a,b), is not exposed but may occur several tens of metres below the base of the section. The exposed sediments have varying and partly high TOC contents, but very low HI values (≤90 mgHC/gTOC; Table 2); in the case of sample IDF-07, this is despite the high alginite content (82 vol.%). This suggests poor conditions for organic matter preservation during the low salinity event, which differs from equivalent sediments at the type locality of the Maikop Group (e.g. Lower Morozkina Balka Formation; Sachsenhofer *et al*., 2017).

Following Weber (1935), the overlying Upper Maikop Formation is divided from base to top into members A (308 m thick), B (23 m) and C (17 m). Members A (avg. 1.82 wt.%) and C (avg. 1.71 wt.%) contain significant amounts of organic matter. Even higher TOC contents (~3-6 wt.%) were reported by Baldermann *et al*. (2020). Despite moderately high TOC contents, HI values are typically low (avg. 121, and 114 mgHC/gTOC), but vary significantly (28-491 mgHC/gTOC). The lack of a good correlation between S2 and TOC values (Fig. 7) indicates that the varying HI values are due to different organic matter types rather than due to a mineral matrix effect (e.g. Langford and Blanc-Valleron, 1990) or due to a constant proportion of inert organic matter (Dahl *et al*., 2004). The generally low HI values are probably related to the negative effect of low sedimentation rates on organic matter preservation (e.g. Stein, 1990). The presence of abundant framboidal pyrite in the sediments and high contents of elemental sulphur in the Maikop extracts indicate that bacteria of the sulphur cycle were important for OM decomposition.

Member A represents the long time interval between the late Solenovian and the Sakaraulian (approximately 13 Ma). The member displays cyclic variations in TOC contents, but the HI shows a uniform upward-decreasing trend between 18 m and 300 m from values of ~200 to ~50 mgHC/gTOC. In addition, slightly elevated TOC contents and HI values are also observed in the uppermost part of the member (303-325 m).

The initial $^{187}Os/^{188}Os$ ratios of high TOC samples with (moderately) high HI values near the base of member A (0.70 ± 0.03) and near its top (0.80 ± 0.14 and 0.56 ± 0.13, Washburn *et al*., 2019) are either higher or lower than that of the contemporaneous global ocean (0.61 ± 0.05 and ~0.72; Peucker-Ehrenbrink and Ravizza, 2020). This indicates that there was limited connectivity between the Eastern Paratethys and the global ocean during deposition of these sediments, and suggests that basin restriction resulted in (slightly) higher organic matter preservation

as reflected by the higher HI values. The reduced salinity of the surface waters during deposition of the uppermost part of member A, suggested by the presence of *Batiacasphaera* sp. (Popov *et al*., 2008), may be another consequence of basin isolation. Salinity stratification is indicated by the presence of a fully-marine fish fauna, which occurred to depths of at least 300 to 400 m (Popov *et al*., 2008).

TOC/S ratios are generally very low in member A, which indicates anoxic conditions (e.g. Berner, 1984). Slightly elevated TOC/S ratios between 195 and 300 m are probably due to weathering of sub-section IDG (Fig. 4d), and should not therefore be used for environmental interpretations. Weathering of the sulphur-rich sediments gives the rocks a yellowish colour in outcrop due to jarosite formation.

The black-coloured member B, 22 m thick, contains surprisingly low amounts of TOC (avg. 0.69 wt.%) and sulphur (avg. 0.28 wt.%). Whereas TOC contents do not show a depth trend, HI values decrease gradually upwards from 60 to 20 mgHC/gTOC suggesting that conditions for OM preservation were poor and deteriorated through time. This interpretation is supported by the observation of strongly corroded palynomorphs in member B (Popov *et al*., 2008).

With the exception of the uppermost samples, TOC/S ratios are high. This reflects low salinity conditions, at least in the surface waters, as suggested by Popov *et al*. (2008) based on the impoverished palynoflora dominated by *Batiacasphaera* sp. Low TOC contents and low HI values show that increasing basin isolation during the middle/late Kozakhurian did not result in improved OM preservation. It should be noted that, based on its black colour, member B has formerly been described as organic-rich (Weber, 1935; Popov *et al*., 2008). However, the new data show that the dark surface colour is due to the absence of jarosite resulting from pyrite weathering, a consequence of the very low sulphur content. Member C is generally poor in organic matter, but includes a few intervals with TOC contents of 2.1 – 5.7 wt.%TOC.

Samples from Maikop sediments with high TOC contents (1.64-5.72 wt.%) and strongly varying HI values (42-491 mgHC/gTOC) were used to determine the OM type based on maceral analysis and biomarkers. High vitrinite percentages show that there was a significant input of terrigenous organic matter into the basin. This agrees with the observation of abundant wood fragments in the Islamdag section reported by Popov *et al*. (2008 *cum lit.*) as well as of silicified wood in member A. Despite this, concentrations of land plant biomarkers (mainly gymnosperm-derived diterpenoids) are low. Moreover, although angiosperm wood has been detected besides the more common gymnosperm wood (Popov *et al*., 2008), angiosperm-derived triterpenoids could not be identified.

Hop-17(21)-ene is present in all samples. Based on its slightly ^{13}C-depleted isotope composition (Table 5), an origin from heterotrophic bacteria is suggested. High steroid/hopanoid ratios suggest that bioproductivity in the photic zone outcompeted bacterial activity.

The *n*-alkane distribution patterns of most samples are dominated by long-chain *n*-alkanes with a marked odd-over-even predominance (e.g. IDF-07; Fig. 9), indicating the contribution of plant waxes (Eglinton and Hamilton, 1967). However, in three samples (IDB-09, IDB-23, IDG-53) near member B, different *n*-alkane distributions were obtained. In these samples, short-chain *n*-alkanes dominate (Fig. 9), indicating high contributions of alkanes derived from algae and/or micro-organisms (Cranwell, 1977). Furthermore, the *n*-alkanes are depleted in ^{13}C compared to the rest of the samples from the Maikop Group (Table 5, Fig. 11c). The data may indicate algal or bacterial blooms in the photic zone of the water column. Short-chain *n*-alkanes have been found to predominate in cultures of cyanobacteria adapted to salinity (NaCl) stress (Bhadauriya *et al*., 2008). Significantly lower steroid/hopanoid ratios suggest accelerated bacterial activity during OM deposition in these samples.

High concentrations of HBIs, especially at 106.90 m (IDF-39) and 188.30 m (IDF-67), indicate high productivity of marine diatoms. HBIs (and *n*-alkanes) in the Maikop Group from the Islamdag section are less depleted in ^{13}C than those in the older sediments in the Perekishkyul section. The presence of diatoms and other siliceous organisms is also indicated by the high biogenic silica contents in samples from the uppermost member A and from member C. HBIs are known exclusively from marine diatoms (Table 4). Hence, the lack of HBIs in these sediments may reflect the low salinity. Unfortunately, the MTTC ratio, a biomarker-based salinity proxy (e.g. Sinninghe Damsté *et al*., 1987), could not be determined. The presence of the 24-norcholestane has been used to trace the contribution of dinoflagellates or diatoms (Holba *et al*., 1998; Rampen *et al*., 2007).

The difference in isotope ratios of pristane and phytane is remarkably high (up to 3.5 ‰) in samples IDF-07, -10, -39 and -67 (13.20-188.30 m; Fig. 11h). This suggests that the phytane peak is overlain by another isotopically-light compound, probably crocetane. Hence, the Pr/Ph ratios determined for these samples (0.11-0.18) should not be used for the assessment of redox conditions. However, the presence of HBI and isoprenoid thiophenes as well as (minor amounts of) DBT suggest highly oxygen-deficient conditions for most studied samples. Minor amounts of crocetane (co-eluting with phytane in the chromatograms) and irregular PMI, as evidenced by their low δ^{13}C values, suggest the presence of methanotrophic archaea beside sulphate-reducing

bacteria in the anoxic part of the water column (Elvert *et al.*, 2000).

Chokrak-Spirialis Formation

Deposition of the Maikop Group sediments ended with the Tarkhanian flooding event, which caused oxygenation of the Eastern Paratethys (Palcu *et al.*, 2019b). The occurrence of the deep-water fish *Vinciquerria merklini* in the lower part of the Chokrak-Spirialis Formation suggests oxic deep-marine conditions which allowed fish populations to survive down to the depth of 700 to 1000 m (Popov *et al.*, 2008). Consequently, TOC contents in the Chokrak-Spirialis Formation are generally low. The first occurrence of (calcareous) *Limacina* sp. (= *Spirialis* sp.) fossils several metres above the base of the Chokrak-Spirialis Formation reflects restricted connection with the open ocean and variable salinities (Popov *et al.*, 2008).

Although the Chokrak-Spirialis Formation in general has TOC contents below 1.5 wt.%, a few samples contain more than 2 wt.%. Sample IDC-48.2 (TOC: 2.37 wt.%; HI: 214 mgHC/gTOC) from the upper part of the formation has been analyzed in detail. This sample contains the highest amount of vitrinite (64 vol.%) within the studied sample set and a very high proportion of long-chain *n*-alkanes (57 %) with a pronounced odd-even predominance (CPI: 5.10). This demonstrates a high proportion of terrigenous organic matter influx, and low amounts of HBI alkanes reflect the (minor) diatom biomass. The very low Pr/Ph ratio (0.18), the presence of PMI and isoprenoid thiophenes, although in low amounts, together with a TOC/S ratio (0.91) which is significantly lower than the average for the formation (2.18), indicate short-term events with strongly oxygen-depleted bottom waters.

Diatom Formation (Paper Shale)

The lithology of the Diatom Formation justifies its subdivision into a lower interval (429-629 m), the middle paper shale interval (590-629 m), and an upper interval (629-750 m). In the lower and upper intervals of the Diatom Formation, TOC contents are very low indicating depositional environments which were not suitable for organic matter accumulation. This also applies for the basal layers, which contain an endemic fish fauna (e.g. *Sardinella karaganica, Mugil karaganicus*) indicating deposition in the Karaganian basin with reduced salinity (Popov *et al.*, 2008; Palcu *et al.*, 2019b). The slightly increased TOC/S ratios (Fig. 5) in the basal part of the Diatom Formation may result from this freshening event.

Detailed investigations were focused on the paper shale interval and its lower and upper transition zones. Although, the Re/Os age of the paper shale has significant uncertainty (7.2 ± 2.6 Ma; Fig. 6B), it

nominally indicates deposition in the late Tortonian/early Messinian; but including the uncertainty, the age range is mid-Tortonian to early Zanclean. However, the absence of Pontian sediments exclude an age younger than 6.1 Ma (van Baak *et al.*, 2016). Irrespective of the precise depositional age, the initial $^{187}Os/^{188}Os$ (0.80 ± 0.02) is slightly lower (less radiogenic) than that observed in the late Miocene global $^{187}Os/^{188}Os$ oceans (~0.85; Peucker-Ehrenbrink and Ravizza, 2020), indicating restriction of the Kura Basin during deposition.

Reflected light microscopy shows that organic matter is dominated by alginite macerals (62-90 vol.%). Lamalginite (including liptodetrinite) is typically more common than telalginite, which dominates over lamalginite only in the lowermost two samples. This suggests that the organic matter is mainly composed of algal or bacterial mats. The relative amount of short-chain *n*-alkanes is negatively correlated with $\delta^{13}C$ values of *n*-C_{19} ($R^2 = 0.54$) suggesting that short-chain *n*-alkanes derived from algal organic matter are isotopically light.

Diatoms are observed frequently in reflected light and SEM photomicrographs (Fig. 8). Considering the abundance of the diatom remains, the concentration of biogenic silica is low (Fig. 8). HBI compounds, characteristic of some (usually marine) diatom assemblages, were not detected (Fig. 10). However, high abundances of C_{28} steradienes which are structurally similar to 24-methylcholesta-5,24(28)-dien-3β-ol and 24-methylcholesta-5,22-dien-3β-ol (brassicasterol) indicate the contribution of diatoms to bioproductivity. The lack of C_{25} HBI alkane suggests differences in diatom assemblages compared to the organic matter in the Upper Maikop Formation.

Apart from aquatic liptinite macerals, detrital vitrinite macerals also occur in significant amounts (6.6 – 35.0 vol.%). The relative amounts of long-chain *n*-alkanes, which correlate well with CPI values ($R^2 = 0.83$ or even 0.90, if sample IDD-52 above the paper shale is neglected) are geochemical indicators for the terrigenous fraction. Thus, it is not surprising that vitrinite percentages correlate positively ($R^2 = 0.50$) with both the amount of long-chain *n*-alkanes and with the CPI. Concentrations of gymnosperm-derived diterpenoids are low. Triterpenoids are not measurable, except arborene which is of controversial origin (e.g. IDD-10); arborane-type triterpenoids may be derived from angiosperms, grasses or bacteria (Hauke *et al.*, 1992). The ^{13}C-enriched isotopic composition (-24.9‰; Table 5) of the C_{30} arborene measured in sample IDD-10 does not support a microbial origin.

PMI and crocetanes occur in enhanced amounts, suggesting the importance of archaea involved in methane cycling (e.g. anoxic methane oxidizers). The diminishing content of 24-*n*-propylcholestane, and
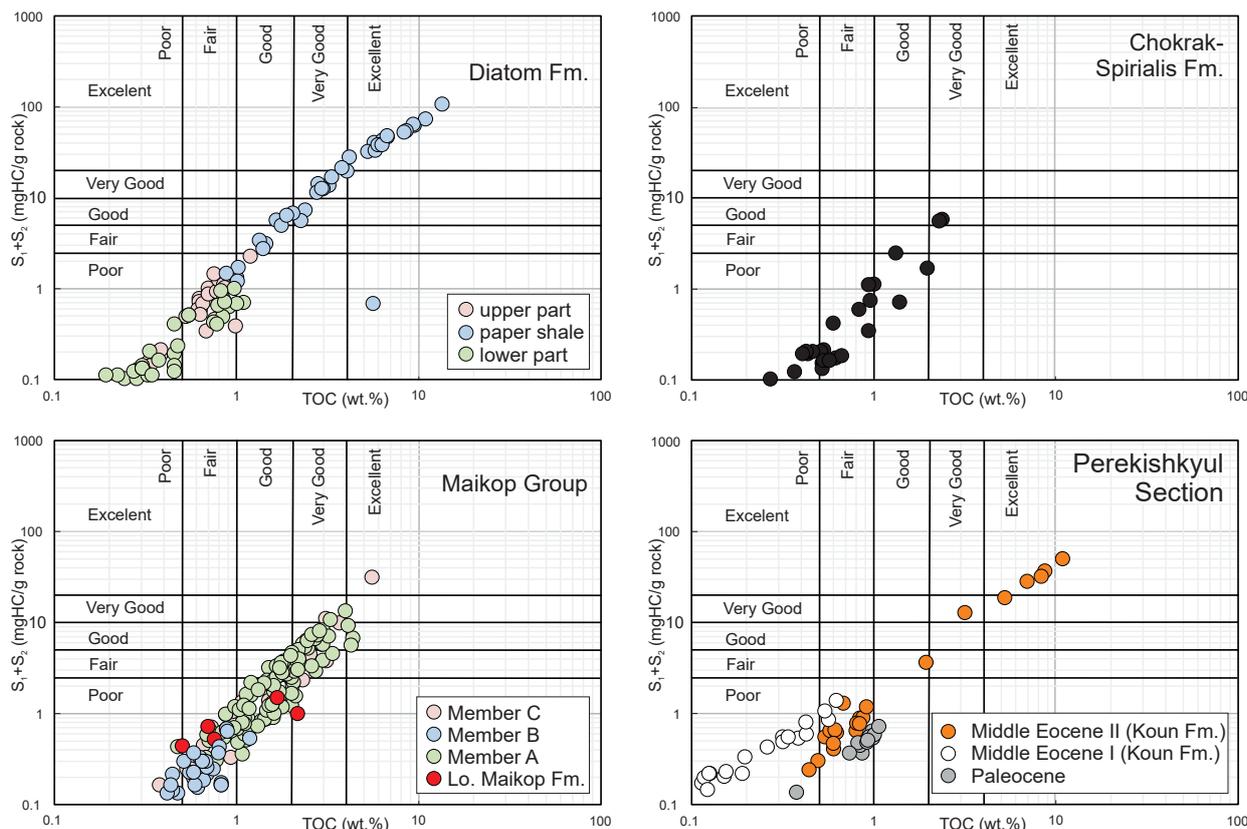
Fig. 12. Plot of TOC versus Rock-Eval (S1+S2) for samples of different stratigraphic units from the Perekishkyul and Islamdag sections.

lower abundances of framboidal pyrite and elemental sulphur in the extracts provide evidence for decreased activity of sulphur cycle bacteria and probably also brackish-water conditions due to freshwater inflow. Reduced salinity, probably related to the limited connectivity between the basin and the global ocean, is also suggested by high TOC/S ratios (avg. 5.24; Table 2). In contrast to sediments of the Maikop Group, C_{30} 4-methylsteranes are present in the rock extracts and are most probably derived from dinoflagellates (Robinson *et al.*, 1984).

The dominance of hydrogen-rich algal material is also reflected by the slope of the regression line in the cross-plot of S2 versus TOC (Fig. 7), which shows that the reactive organic matter (*sensu* Dahl *et al.*, 2004) in all paper shale samples has an average HI of 764 mgH/gTOC (kerogen Type I/II). The positive intercept of the regression line shows that the inert organic matter fraction is about 1.1 wt.%. Hence, varying HI values reflect different relative contributions of algal and inert organic matter.

Strictly anoxic conditions during deposition of the paper shale interval are proven by the preservation of sediment lamination, the excellent preservation of organic matter, and biomarker proxies (e.g. PMI, crocetane). Hence, oxic conditions, as postulated recently by Abdullayev *et al.* (2021) based on redox-sensitive elements, can be excluded.

Petroleum Potential

In this section, the petroleum potential of the sediments studied in the Perekishkyul and Islamdag sections is discussed using cross-plots of the generation potential (Rock-Eval S1+S2) versus TOC content (Fig. 12). The potential of stratigraphic units which are not exposed in the study area will be evaluated in a following section below.

Paleocene sediments in the Perekishkyul section contain moderately high TOC contents (avg. 0.90 wt.%) with very low HI values. Although this unit contains surprisingly high percentages of alginite, it does not hold any commercial source-rock potential. The same applies for the Middle Eocene I sediments which are exposed in the same section (see Fig. 12).

Within the upper part of the Perekishkyul section (Middle Eocene II), very good to excellent petroleum potential is limited to cm-thick, organic-rich intervals that occur within dm-thick, low-TOC successions. The determined high (true) HI of 412 mgHC/gTOC (Fig. 7) shows that the sediments are oil prone. As mentioned above, the cumulative thickness of the organic-rich layers is difficult to determine but probably does not exceed 2 m. Assuming a net thickness of 2 m and an average density of 2.3 t/m³ for the largely carbonate-free sediments results in an SPI value of 0.11 t/m². This shows that the hydrocarbon potential of the middle Eocene in the study area is very low.

Based on the TOC contents, a good to very good petroleum potential can be attributed to members A and C in the Islamdag section, whereas member B has only fair potential (Fig. 12). However, as the generation potential (S1+S2) is typically low (Table 2), the Maikopian sediments have only fair to good petroleum potential. This discrepancy between high TOC contents and low generation potential is reflected by low HI values indicating the prevalence of Type II-III kerogen. Hence, the Maikopian sediments in the Islamdag section are oil- to gas-prone. The SPI (Demaison and Huizinga, 1991) has been calculated for members A and C, while member B is not considered a potential source rock of significance. Assuming an average density of 2.3 t/m³, the SPI is determined as 1.98 and 0.12 tons of hydrocarbons/m² for members A and C, respectively. Thus, the upper Solenovian to lower Miocene part of the Maikop Group may generate a total of 2.10 tHC/m². The hydrocarbon potential of the Pshekhian and lower Solenovian part of the Maikop Group remains unknown. However, data from the Siyaki (Pshekhian) and Shikhzairli (lower Solenovian) sections located to the west of Mount Islamdag (Saint-Germès, 1998) suggest that the Pshekhian and lower Solenovian could probably contribute an additional 0.28 and 0.05 tHC/m² to the entire Maikop Group. Thus, the Maikop Group in the Islamdag area may generate about 2.5 tHC/m². This total is of the same order as that suggested by Sachsenhofer *et al.* (2018b) for the Maikop Group in Azerbaijan.

The Chokrak-Spirialis Formation deposited after the Tarkhanian flooding event contains layers with high TOC contents, and a few samples can be classified as good source rocks (Fig. 12). However, the average generation potential is low (0.82 mg HC/g rock) and the formation is not considered a potential source rock.

In the Diatom Formation, whereas the intervals below and above the paper shales cannot be considered as potential source rocks, the paper shale interval itself (590-629 m) comprises highly oil-prone source rocks with good to excellent petroleum potential (Fig. 12). The SPI of the paper shale interval has been calculated for rock densities of 2.0 t/m³ (2.89 tHC/m²) and 2.3 t/m³ (3.33 tHC/m²). The values obtained show that independent of the applied rock density, and despite the significantly lower thickness of the paper shale, its hydrocarbon potential is higher than that of the Maikop Group. Considering the differences in generation potential, the expulsion efficiency of the paper shale is also probably much higher than that of the Maikop Group (cf. Mackenzie and Quigley, 1988).

Distinguishing the oils generated by the Maikop Group and the Diatom Formation

It is widely accepted that the Maikop Group and the Diatom Formation are the main source rocks in the South Caspian Basin (e.g. Wavrek *et al.*, 1998; Smith-Rouch, 2006; Goodwin *et al.*, 2020), although it is not clear whether the Diatom Formation has reached oil window maturity (Inan *et al.*, 1997). Therefore, it is useful to check if isotope and/or biomarker data allow a distinction to be made between the oils generated by these stratigraphic units.

A systematic decrease of $\delta^{13}C$ values of the saturated and aromatic hydrocarbon fractions with stratigraphic age has been reported by Abrams and Narimov (1997). Whereas extracts from Lower Oligocene source rocks are isotopically light ($\delta^{13}C_{sat}$: ~-28‰; $\delta^{13}C_{aro}$: ~-28‰), extracts from the Diatom Formation are relatively enriched in ^{13}C ($\delta^{13}C_{sat}$: ~-23‰; $\delta^{13}C_{aro}$: ~-24‰). Using compound specific isotope data of *n*-alkanes, a similar trend was observed for the lower and upper Oligocene sediments at Angeheran (for location see Fig. 1; Bechtel *et al.*, 2013).

Lowermost Oligocene sediments are not exposed in the studied sections. Hence, the complete stratigraphic succession of the Maikop Group could not be investigated. However, results from the part of the Maikop Group exposed in the Islamdag section (upper Solenovian to lower Miocene; Fig. 11b-d) show more differentiated results with strongly varying compound specific isotope data, especially in the lower Miocene (Kozakhurian) sediments (Fig. 11c). Moreover, no systematic difference in the $\delta^{13}C$ isotopic composition of *n*-alkanes exists between the investigated upper Oligocene to lower/middle Miocene samples from the Maikop Group and the Diatom Formation (Fig. 11e-f). Hence, it might be possible to distinguish middle Eocene oils from upper Solenovian to Miocene oils, but based on isotope data alone it is impossible to distinguish oils derived from the Upper Maikop Formation and the Diatom Formation.

In contrast to the carbon isotope data, there are differences in the presence of specific biomarkers between the samples of the Maikop Group and the Diatom Formation paper shales. The investigated samples from the Diatom Formation contain C_{30} 4-methylsteranes in elevated contents and no C_{30} steranes, whereas the rest of the sample set is characterized by the presence of 24-*n*-propylsterane with lower amounts of methylsteranes. The generated oils should therefore differ in the presence of methylsteranes (paper shales) versus the presence of additional C_{30} steranes (Maikop Group, Middle Eocene II). Furthermore, the C_{25} HBI compounds (alkane and thiophenes) were exclusively found in the extracts from samples of the Maikop Group (and the Middle Eocene II), and early-generated oils from the Maikop Group should therefore include the C_{25} HBI alkane. The oils derived from the Diatom Formation may be also distinguished by the higher relative contributions of the C_{25} isoprenoid (PMI).

Implications for source rock distribution in Azerbaijan and the Eastern Paratethys

The Perekishkyul and Islamdag sections provide information on the stratigraphic distribution of source rocks in Paleocene and middle Eocene intervals and in a largely continuous lower Oligocene to upper Miocene succession. However, there are gaps in sedimentation between the Paleocene and middle Eocene in the Perekishkyul section, as well as between the middle Eocene and the upper Solenovian in the Islamdag section (Fig. 2). The possibility of the presence of organic-rich horizons within these identified stratigraphic gaps is discussed in this section, together with the lateral distribution of organic-rich intervals with the upper Middle Eocene II and the paper shale interval in the Diatom Formation.

With the exception of thin layers in the upper part of the middle Eocene (Middle Eocene II), Paleocene and Eocene sediments in the Perekishkyul section are poor source rocks. However, three prominent black shale horizons may be present in the Paleocene to Eocene succession that appear to be missing in the studied sections. These include sediments deposited during the Paleocene/Eocene thermal maximum (PETM) and the Early Eocene Climatic Optimum (EECO), as well as the middle Eocene Kuma Formation (see Fig. 2 for stratigraphic positions).

PETM sediments deposited in the northeastern Peri-Tethys are often only a few decimetres thick, but can be traced from Crimea to Central Asia (Gavrilov *et al*., 2003; 2018). In Crimea and the northwestern Caucasus foreland, these sediments contain low amounts of organic matter (Gavrilov *et al*., 2018). Elsewhere, including in the Rioni Basin in Georgia and in the central and northeastern Caucasus foreland, they are rich in organic matter and TOC contents may exceed 10 wt.% (Gavrilov *et al*., 2003; 2019). HI values may reach 500 mgHC/gTOC near the base of the sapropelic interval but are more typically low (Gavrilov *et al*., 2009; Shcherbinina *et al*., 2016). Similarly, sapropelic intervals related to the Early Eocene Climatic Optimum (EECO), 7 to 30 cm thick, occur in the marly lower Eocene (Ypresian) succession in the northern Caucasus (e.g. Shcherbinina *et al*., 2020). Although it is likely that both horizons are present near the eastern end of the Greater Caucasus, to the authors' knowledge neither PETM nor EECO sediments have been described in Azerbaijan.

The middle Eocene Kuma Formation comprises organic-rich marly rocks which were deposited in a dysoxic to anoxic basin extending from Crimea to the Aral Sea (Beniamovski *et al*., 2003). It has been suggested that volcanic material contributed to the increased organic matter content (Vincent and Kaye, 2017). The succession, several tens of metres thick, is a prolific hydrocarbon source rock in Georgia and

southern Russia (Sachsenhofer *et al*., 2018b; 2021 *this issue*; Oblasov *et al*., 2020). Time equivalents of this formation have likewise not yet been described in Azerbaijan. "Oil shale layers" within the middle part of the Koun Formation mentioned in previous publications (e.g. Abbasov, 2005) may correlate with the Kuma Formation. However, the available data are not adequate to judge either the age of the sediments or the amount and type of organic matter. The Eocene part of the Perekishkyul section is generally poor in organic matter, but includes cm-thick layers with high TOC contents. As new radiometric age data suggest a middle Eocene age, these layers may represent equivalents of the Kuma Formation. In contrast to the Kuma Formation, the organic-rich layers in the Perekishkyul section are thin and interbedded with largely carbonate-free claystones, whereas marly interbeds are restricted to the upper part of the succession. Similar sediments, about 14 m thick, have been described from outcrops 5 km south of the Sumgait railway station (Saint-Germès, 1998; for location see Fig. 1). This suggests that the interval containing thin organic-rich layers within the Middle Eocene II unit is laterally persistent. The net thickness of the organic-rich layers is difficult to determine but is probably below 2 m, suggesting that the source rock potential is minor (~0.1 tHC/m²). However, there may be an increase in the thickness of these layers towards the South Caspian Basin.

Another major stratigraphic gap exists between the top of the Middle Eocene II (~38 Ma) and the base of the Islamdag section (~30 Ma; Fig. 2). The lowermost carbonate-free sediments in the Islamdag section were deposited following the low-salinity "Solenovian Event" (e.g. Popov *et al*., 2004). Elsewhere in the Eastern Paratethys, the Solenovian Event is represented by a carbonate-rich layer (e.g. the Ostracoda (= Polbian) Bed) overlain by shaly sediments that have the highest hydrocarbon potential of the entire Maikop Group (Sachsenhofer *et al*., 2017; 2018a,b). Until now, the Ostracoda Bed has not been described in the Lower Kura Basin of Azerbaijan, but a short section (~7 m) with low carbonate sediments attributed to the Solenovian Event based on palynological data has been described from an outcrop 2 km south of Shikhzairli (Akhmetiev *et al*., 2007; for location see Fig. 1). TOC contents (0.33-0.73 wt.%) and HI values (61-182 mgHC/gTOC) of these samples are low (Saint-Germès, 1998).

Source rock parameters of lower Oligocene sediments were also investigated near Siyaki, Angeheran and Lahich. However, none of these sections provided evidence for the presence of the Solenovian Event (Saint-Germès, 1998; Bechtel *et al*., 2013, 2014). Thus, the source rock potential of (Pshekhian and) lower Solenovian sediments in the Lower Kura Basin of Azerbaijan remains unclear.

Major parts of the lower Oligocene (upper Solenovian) to middle Miocene (Kozakhurian) part of the Maikop Group have fair to good petroleum potential. It is not disputed that these sediments are of wide lateral extent. Moreover, higher sedimentation rates in the South Caspian Basin to the east may have resulted in improved organic matter preservation and the increased generation potential of the Maikop Group.

The thickness of the Maikop Group in the Eastern Paratethys varies significantly. For example, its thickness increases from about 600 m in the Sea of Azov to more than 4 km in the Taman peninsula (Popov *et al*., 2019). Similarly, the thickness of the Maikop Group increases dramatically from onshore areas to the South Caspian Sea (Green *et al*., 2009). However, thickness variations are also observed within the Lower Kura Basin. Lower Oligocene sediments, about 700 m thick, occur near Lahich (Fig. 1a; Bechtel *et al*., 2014). In contrast, the thickness of the lower Oligocene succession near Angeheran is only some 175 m. The lower Oligocene succession at these sites was deposited in a strongly oxygen-depleted environment (Bechtel *et al*., 2013, 2014). Consequently, the source rock quality is relatively good (~3 wt.% TOC; HI ~300 mgHC/gTOC). In contrast, upper Oligocene rocks at Angeheran, more than 250 m thick, are poor source rocks (Bechtel *et al*., 2013). This may indicate that the source rock quality of upper Oligocene (and lower Miocene) units increases eastwards.

The exposed part of the Diatom Formation in the Islamdag section is 320 m thick. Most of the sediments have low TOC contents (429-629 m; 688-750 m), but a 59 m thick interval of paper shales with very high TOC contents and HI values occurs about 250 m above the base of the formation. Both Khersonian and Maeotian ages for these black shales are possible. The great variability of source rock properties of samples of the Diatom Formation has been noted previously (Feyzullayev *et al*., 2001; Alizadeh *et al*., 2017). However, based on the characteristics of rock samples ejected from mud volcanoes in the Shamakhy-Gobustan area and of cores from boreholes located south of Baku (Baku archipelago), Feyzullayev *et al*. (2001) assumed that the petroleum potential of the Diatom Formation increases with depth and to the south (see also Alizadeh *et al*., 2017). Hence, marked variations in petroleum potential were interpreted in terms of lateral facies variability. The presence of a single organic-rich black shale horizon within organic-poor sediments of the Diatom Formation, which is evident in the Islamdag section, has seemingly so far been overlooked. Middle Miocene "oil shales" with Konkian to Maeotian ages were mentioned by Abbasov (2015). Furthermore, it is possible that the 14 m thick succession at Gezdek with TOC contents exceeding 10

wt.% and HI values up to 800 mgHC/gTOC, described as consisting of lower Miocene Maikopian sediments (Katz *et al*., 2000), belongs to the Diatom Formation. For an improved understanding of the petroleum system, it will be important to understand the lateral distribution of these intervals.

No new source rock data are available for fine-grained intervals within the lower Pliocene Productive Series. However, Alizadeh *et al*. (2017) showed that TOC contents (average 0.47 wt.%; max. 2.71 wt.%) and HI values (average 147 mg HC/g rock; max. 334 mg HC/g rock) are typically low.

CONCLUSIONS

This study of Paleocene to Miocene sediments exposed in the Perekishkyul and Islamdag sections in the Gobustan area west of Baku provides new information on the distribution and quality of source rocks in eastern Azerbaijan and the South Caspian Basin. In addition, it helps us to understand changes in the regional palaeodepositional environment during Oligocene and Miocene times. The very low thermal maturity of the samples analysed may influence some biomarker ratios (e.g. the Pr/Ph and diasterane/sterane ratios) which can be used as environmental proxies. The most important results of the study are as follows:

The upper part of the middle Eocene succession (Middle Eocene II) includes an approximately 40 m thick interval composed of alternations of decimetre-thick organic-poor layers and cm-thick organic-rich layers. The latter contain very large amounts of kerogen Type II with abundant marine organisms. Similar alternations have been described from several outcrops and are probably of significant lateral extent. Because of the low net thickness of the organic-rich layers, the middle Eocene cannot be considered as a significant source rock in onshore eastern Azerbaijan.

The exposed part of the Maikop Group in the Islamdag section is 364 m thick. A new Re/Os age from the base of the Group in this section (30.0 ± 1.0 Ma) shows that the exposed sediments were deposited during early Oligocene (late Solenovian) to middle Miocene times, and that sedimentation rates were low (~25 m/Ma). Low sedimentation rates related to the deep-marine setting promoted organic matter degradation. The lowermost sediments represent the uppermost layers of the Solenovian Event. TOC contents are often high, but HI values are typically low (kerogen Type II/III). The Maikop Group (including the Pshekhian and lower Solenovian units) could generate about 2.5 tHC/m². Apart from the dominant aquatic micro-organisms (including diatoms, methanotrophic archaea and sulphate-reducing bacteria), the organic matter includes varying amounts of terrigenous land plant material.

The Diatom Formation includes a paper shale interval, about 60 m thick, with very high TOC contents (max. 13.3 wt.%) and HI values (max. 770 mgHC/gTOC; kerogen Type II-I). This interval may generate more hydrocarbons than the Maikop Group (~3 t/m²). The organic material is dominated by algae (including diatoms) deposited in a basin with reduced salinity. Strictly anoxic conditions are indicated by the presence of biomarkers for archaea involved in methane cycling. Dinoflagellates also contributed to the biomass.

Carbon isotope data allow a distinction to be made between oil generated from middle Eocene source rocks, and that from upper Solenovian to upper Miocene source rocks. Oil generated from the Maikop Group and the paper shales within the Diatom Formation can be distinguished based on the presence of specific biomarkers. For example, oils generated from the Maikop Group should include C_{30} steranes and C_{25} HBI compounds (alkane and thiophene) that are absent in oils generated by the paper shales. The oils derived from Diatom Formation may be also distinguished by the higher relative contributions of the C_{25} isoprenoid (PMI) and of C_{30} methylsteranes.

ACKNOWLEDGEMENTS

Data availability statement
The data that support the findings of this study are available from the corresponding author upon reasonable request.

REFERENCES

ABBASOV, O.R., 2015. Oil shale of Azerbaijan: Geology, geochemistry and probable reserves. *International Journal of Engineering and Technology,* **2**, 31-37.

ABDULLAYEV, E., BALDERMANN, A., WARR, L. N., GRATHOFF, G. AND TAGHIYEVA, Y., 2021. New constraints on the palaeo-environmental conditions of the Eastern Paratethys: Implications from the Miocene Diatom Suite (Azerbaijan). *Sedimentary Geology,* **411**, 105794.

ABRAMS, M.A. AND NARIMOV, A.A., 1997. Geochemical evaluation of hydrocarbons and their potential sources in the western South Caspian depression, Republic of Azerbaijan. *Marine and Petroleum Geology,* **14**, 451-568.

AKHMETIEV, M.A., ZAPOROZHETS, N.I., GOLOVINA, L.A., POPOV, S.V., SYCHEVSKAYA, E.K., EFENDIYEVA, M.A., FEYZULLAYEV, A.A. AND ALIYEV, Ch.S., 2007. New Data on Stratigraphy of the Maikop Group in Central Gobustan. *Stratigraphy and Sedimentology of Oil and Gas Basins,* **1**, 32–53 [in Russian].

ALIZADEH, A.A., GULIYEV, I.S., KADIROV, F.A. AND EPPELBAUM, L.V., 2017. Geosciences of Azerbaijan. Vol. 2: Economic Geology and Applied Geophysics, Springer, 340 pp.

BALDERMANN, A., ABDULLAYEV, E., TAGHIYEVA, Y., ALASGAROV, A. AND JAVAD-ZADA, Z., 2020. Sediment petrography, mineralogy and geochemistry of the Miocene Islam Dag Section (Eastern Azerbaijan): implications for the evolution of sediment provenance, palaeo-environment and (post-)depositional alteration patterns. *Sedimentology,* **67**, 152-172, doi: 10.1111/sed.12638.

BATI, Z., 2015. Dinoflagellate cyst biostratigraphy of the upper Eocene and lower Oligocene of the Kirmizitepe Section, Azerbaijan, South Caspian Basin. *Review of Palaeobotany and Palynology,* **217**, 9–38. http://dx.doi.org/10.1016/j.revpalbo.2015.03.002.

BECHTEL, A., GRATZER, R., SACHSENHOFER, R.F., GUSTERHUBER, J., LÜCKE, A. and PÜTTMANN, W., 2008. Biomarker and carbon isotope variation in coal and fossil wood of Central Europe through the Cenozoic. *Palaeogeography, Palaeoclimatology, Palaeoecology,* **262**, 166-175.

BECHTEL, A., MOVSUMOVA, U., STROBL, S.A.I., SACHSENHOFER, R.F., SOLIMAN, A., GRATZER, R. AND PÜTTMANN, W., 2013. Organofacies and paleoenvironment of the Oligocene Maikop series of Angeharan (eastern Azerbaijan). *Organic Geochemistry* **56**, 51-67.

BECHTEL, A., MOVSUMOVA, U., PROSS, J., GRATZER, R., CORIC, S. AND SACHSENHOFER, R.F., 2014. The Oligocene Maikop series of Lahich (eastern Azerbaijan): Paleoenvironment and oil-source rock correlation. *Organic Geochemistry* **71**, 43-59.

BENIAMOVSKI, V.N., ALEKSEEV, A.S., OVECHKINA, M.N. AND OBERHÄNSLI, H., 2003. Middle to upper Eocene dysoxic-anoxic Kuma Formation (northeast peri-Tethys): biostratigraphy and paleoenvironments. *Geol. Soc. Am. Spec. Paper,* **369**, 95–112.

BERNER, R.A., 1984. Sedimentary pyrite formation: An update. *Geochimica et Cosmochimica Acta,* **48**, 605-615, doi:10.1016/0016-7037(84)90089-9.

BHADAURIYA, P., GUPTA, R., SINGH, S. AND BISEN, P.S., 2008. n-Alkanes variability in the diazotrophic cyanobacterium Anabaena cylindrica in response to NaCl stress. *World Journal of Microbiology and Biotechnology,* **24**, 139-141.

BIRGEL, D., THIEL, V., HINRICHS, K.-U., ELVERT, M., CAMPBELL, K.A., REITNER, J., FARMER, J.D. AND PECKMANN, J., 2006. Lipid biomarker patterns of methane-seep microbialites from the Mesozoic convergent margin of California. *Organic Geochemistry,* **37**, 1289-1302.

BOOTE, D.R.D., SACHSENHOFER, R.F., TARI, G. AND ARBOUILLE, D., 2018. Petroleum provinces of the Paratethyan region. *Journal Petroleum Geology,* **41**, 247-298. doi: 10.1111/jpg.12703.

COPLEN, T.B., 2011. Guidelines and recommended terms for expression of stable-isotope-ratio and gas-ratio measurement results. *Rapid Communications in Mass Spectrometry,* **25**, 2538–2560. https://doi.org/10.1002/rcm.5129.

CRANWELL, P. A., 1977. Organic geochemistry of CamLoch (Sutherland) sediments. *Chemical Geology,* **20**, 205-221.

CREASER, R.A., PAPANASTASSIOU, G.J. AND WASSERBURG, G.J., 1991. Negative thermal ion mass spectrometry of osmium, rhenium, and iridium. *Geochimica et Cosmochimica Acta,* **55**, 397-401.

CUMMING, V.M., POULTON, S.W., ROONEY, AD. AND SELBY, D., 2013.

Anoxia in the terrestrial environment during the Late Mesoproterozoic. *Geology*, **41**, 583-586. doi:10.1130/G34299.1

DAHL, B., BOJESEN-KOEFOED, J., HOLM, A., *et al.*, 2004. A new approach to interpreting Rock-Eval S2 and TOC data for kerogen quality assessment. *Organic Geochemistry*, **35**, 1461–1477. https://doi.org/10.1016/j.orggeochem.2004.07.003

DEMAISON, G. AND HUIZINGA, B.J., 1991. Genetic classification of petroleum systems. *AAPG Bulletin*, **75**, 1626–1643.

DIDYK, B.M., SIMONEIT, B.R.T., BRASSELL, S.C. AND EGLINTON, G., 1978. Organic geochemical indicators of palaeoenvironmental conditions of sedimentation. *Nature*, **272**, 216–222.

EGLINTON, G. and HAMILTON, R.J., 1967. Leaf epicuticular waxes. *Science* **156,** 1322-1335.

ELVERT, M., SUESS, E., GREINERT, J. AND WHITICAR, M.J., 2000. Archaea mediating anaerobic methane oxidation in deep-sea sediments at cold seeps of the eastern Aleutian subduction zone. *Organic Geochemistry*, **31**, 1175-1187.

ESPITALIÉ, J., MADEC, M., TISSOT, B., MENNIG, J.J. AND LEPLAT, P., 1977. Source rock characterization method for petroleum exploration. *Offshore Technology Conference*. doi: 10.4043/2935-MS

ESPITALIÉ, J., MAKADI, K.S. AND TRICHET, J., 1984. Role of the mineral matrix during kerogen pyrolysis. *Organic Geochemistry*, **6,** 365-382. doi: 10.1016/0146-6380(84)90059-7

FEYZULLAYEV, A., GULIYEV, I. AND TAGIYEV, M., 2001. Source potential of the Mesozoic-Cenozoic rocks in the South Caspian Basin and their role in forming the oil accumulations in the Lower Pliocene reservoirs. *Petroleum Geoscience* **7**, 409-417.

GAVRILOV, Y.O., SHCHERBININA, E. AND OBERHÄNSLI, H., 2003. Paleocene-Eocene boundary events in the northeastern Peri-Tethys. *Geol. Soc. Am. Spec. Paper*, **369**, 147–168.

GAVRILOV, Y.O, SHCHERBININA, E., GOLOVANOVA, O. AND POKROVSKY, B. 2009. A variety of PETM record in different settings, northeastern Peri-Tethys. Climatic and Biotic Events of the Paleogene 2009, Extended Abstracts, 66-69.

GAVRILOV, Y.O., SHCHEPETOVA, E.V., SHCHERBININA, E.A., GOLOVANOVA, O.V., NEDUMOV, R.I. and POKROVSKY, B.G., 2017. Sedimentary environments and geochemistry of Upper Eocene and Lower Oligocene rocks in the NE Caucasus. *Lithology and Mineral Resources*, **52**, 447-466.

GAVRILOV, Y.O., GOLOVANOVA, O.V., SHCHEPETOVA, E.V. and POKROVSKY, B.G., 2018. Lithological and Geochemical Characteristics of the Paleocene/Eocene Sediments corresponding to the PETM Biospheric Event in the Eastern Crimea (Nasypnoe Section). *Lithology and Mineral Resources*, **53**, 337-348.

GAVRILOV, Y.O, SHCHERBININA, E. and ALEKSANDROVA, G.N., 2019. Mesozoic and Early Cenozoic Paleoecological Events in the Sedimentary Record of the NE Peri-Tethys and Adjacent Areas: An Overview. *Lithology and Mineral Resources,* **54**, 524-543.

GOODWIN, N.R.J., ABDULLAYEV, N., JAVADOVA, A., VOLK, H. AND RILEY, G., 2020. Diamondoids and basin modelling reveal one of the world´s deepest petroleum systems, South Caspian Basin, Azerbaijan. *Journal of Petroleum Geology*, **43,** 133-150.

GRADSTEIN, F.M., OGG, J.G. SCHMITZ, M.D. AND OGG, G.M. (Eds.), 2020. Geologic time scale 2020, Boston, Elsevier, v. 2, 1390 pp.

GREEN, T., ABDULLAYEV, N., HOSSACK, J., RILEY, G. AND ROBERTS, A.M., 2009. Sedimentation and subsidence in the South Caspian Basin, Azerbaijan. In: Brunet, M.F., Wilmsen, M. and Granath, J.W. (Eds), South Caspian to Central Iran Basins. *Geological Society London Special Publication,* **312**, 241–260.

GREENWOOD, P.F. AND SUMMONS, R.E., 2003. GC–MS detection and significance of crocetane and pentamethylicosane in sediments and crude oils. *Organic Geochemistry*, **34,** 1211-1222.

GULIYEV, I.S., TAGIYEV, M.F. AND FEYZULLAYEV, A. A., 2001a. Geochemical Characteristics of Organic Matter from Maikop Rocks of Eastern Azerbaijan. *Lithology and Mineral*

Resources, **36,** 280-285.

HAUKE, V., GRAFF, R., WEHRUNG, P., TRENDEL, J.M., ALBRECHT, P., RIVA, A., HOPFGARTNER, G., GULACAR, F.O., BUCHS, A. AND EAKIN, P.A., 1992. Novel triterpene-derived hydrocarbons of the arborane/fernane series in sediments: Part II. *Geochimica et Cosmochimica Acta*, **56**, 3595-3602.

HINDS, D.J., ALIYEVA, E., ALLEN, M.B., DAVIES, C.E., KROONENBERG, S.B., SIMMONS, M.D. AND VINCENT, S.J., 2004. Sedimentation in a discharge dominated fluvial-lacustrine system: the Neogene Productive Series of the South Caspian Basin, Azerbaijan. *Marine and Petroleum Geology,* **21**, 613-638.

HOLBA, A.G., TEGELAAR, E.W., HUIZINGA, B.J., MOLDOWAN, J.M., SINGLETARY, M.S., MCCAFFREY, M.A. AND DZOU, L.I.P., 1998. 24-Norcholestanes as age-sensitive molecular fossils. *Geology,* **26**, 783-786.

HUDSON, S.M., JOHNSON, C.L., EFENDIYEVA, M.A., ROWE, H.D., FEYZULLAYEV, A.A. AND ALIYEV, C.S., 2008. Stratigraphy and geochemical characterization of the Oligocene-Miocene Maikop series: Implications for the paleogeography of Eastern Azerbaijan. *Tectonophysics* **451**, 40-55.

HUDSON, S.M., JOHNSON, C.L. AND AFANDIYEVA, M.A., 2016. Spatial and temporal variability of Paleocene–Miocene organofacies of the Kura Basin, eastern Azerbaijan, and implications for basin evolution and petroleum generation. *Organic Geochemistry*, **97**, 131-147.

HUGHES, W.B., HOLBA, A.G. AND DZOU, L.I.P., 1995. The ratios of dibenzothiophene to phenanthrene and pristane to phytane as indicators of depositional environment and lithology of petroleum source rocks. *Geochimica et Cosmochimica Acta*, **59**, 3581-3598.

INAN, S., YALCI, N.M., GULIEV, I.S., KULIEV, K. AND FEIZULLAYEV, A.A., 1997. Deep petroleum occurrences in the Lower Kura Depression, South Caspian Basin, Azerbaijan: an organic geochemical and basin modeling study. *Marine and Petroleum Geology,* **14**, 731-762.

ISAKSEN, G.H., ALIYEV, A., BARBOZA, S.A., PULS, D., AND GULIYEV, I., 2007. Regional evaluation of source rock quality in Azerbaijan from the geochemistry of organic-rich rocks in mud-volcano ejecta. In: Yilmaz, P.O. and Isaksen, G.H., (Eds), Oil and gas of the Greater Caspian area. *AAPG Studies in Geology*, **55**, 51-64.

JOHNSON, C.L., HUDSON, S.M., ROWE, H.D. AND EFENDIYEVA, M.A., 2010. Geochemical constraints on the Palaeocene-Miocene evolution of eastern Azerbaijan, with implications for the South Caspian basin and eastern Paratethys. *Basin Research,* **22**, 733–750.

KATZ, B., RICHARDS, D., LONG, D. AND LAWRENCE, W., 2000. A new look at the components of the petroleum system of the South Caspian Basin. *Journal of Petroleum Science and Engineering* **28,** 161-182.

KHALILOV, D.M., 1962. Microfauna and Stratigraphy of Azerbaijan Maikop Series. Akad. Nauk Azerbaidzhan, Baku. 326 p. (in Russian).

KUTUZOV, I., ROSENBERG, Y.O., BISHOP, A. AND AMRANI, A., 2020. The Origin of Organic Sulphur Compounds and Their Impact on the Paleoenvironmental Record. In: Wilkes, H. (Ed.) Hydrocarbons, Oils and Lipids: Diversity, Origin, Chemistry and Fate. Handbook of Hydrocarbon and Lipid Microbiology. Springer, Cham, pp. 355-408. https://doi.org/10.1007/978-3-319-90569-3_1.

LANGFORD, F.F. AND BLANC-VALLERON, M.-M., 1990. Interpreting Rock–Eval pyrolysis data using graphs of pyrolyzable hydrocarbons versus total organic carbon. *AAPG Bulletin,* **74**, 799–804.

LUDWIG, K.R., 1980. Calculation of uncertainties of U-Pb isotope data. *Earth and Planetary Science Letters*, **46**, 212–220.

LUDWIG, K., 2011. Isoplot, Version 4.15: A Geochronological Toolkit for Microsoft Excel. *Berkley Geochronology Centre Special Publication* **4**.

MACKENZIE, A.S. AND QUIGLEY, T.M., 1988. Principles of Geochemical

Prospect Appraisal. *AAPG Bulletin*, **72**, 399-415.

Misch, D., Loucks, J., Gross, D., Mayer-Kiener, V., Mendez-Martin, F., Schmatz, J. and Sachsenhofer, R.F., 2018. Factors controlling shale microstructure and porosity: a case study on Upper Visean Rudov Beds from the Ukrainian Dniepr-Donets Basin. *AAPG Bulletin*, **102**, 2629-2654. https://doi.org/10.1306/05111817295.

Moldowan, J.M., Fago, F.J., Lee, C.J., Jacobson, S.R., Watt, D.S., Slougui, N.E., Jeganathan, A. and Young, D.C., 1990. Sedimentary 24-n-cholestanes, molecular fossils diagnostic of marine algae. *Science*, **247**, 309-312.

Neumeister, S., Gratzer, R., Algeo, T.J., Bechtel, A., Gawlick, H.-J., Newton R. and Sachsenhofer, R.F., 2015. Oceanic response to Pliensbachian and Toarcian magmatic events: Implications from an organic-rich basinal succession in the NW Tethys. *Global and Planetary Change*, **126**, 62-83.

Oblasov, N.V., Goncharov, I.V., Derduga, A.V. and Kunitsyna, I.V., 2020. Genetic Types of Crude Oil in the Eastern Part of the Crimea–Caucasus Area. *Geochemistry International*, **58**, 1278-1298.

Palcu, D.V., Vasilieva, I., Stoica, M. and Krijgsman, W., 2019a. The end of the Great Khersonian Drying of Eurasia: Magnetostratigraphic dating of the Maeotian transgression in the Eastern Paratethys. *Basin Research*, **31**, 33-58.

Palcu, D.V., Popov, S.V., Golovina, L.A., Kuiper, K.F., Liu, S. and Krijgsman, W., 2019b. The shutdown of an anoxic giant: Magnetostratigraphic dating of the end of the Maikop Sea. *Gondwana Research*, **67**, 82-100.

Peters, K.E., Walters, C.C. and Moldowan, J.M., 2005. The Biomarker Guide, Biomarkers and Isotopes in Petroleum Exploration and Earth History, vols. 1 & 2. Cambridge University Press, New York, NY.

Peucker-Ehrenbrink, B. and Ravizza, G., 2020. Osmium isotope stratigraphy. In: Gradstein, F. M., Ogg, J.G., Schmitz, M.D. and Ogg, G. M. (Eds), The Geologic Time Scale 2020. DOI: 10.1016/B978-0-12-824360-2.00008-5

Popov, S.V., Rögl, F., Raznov, A.Y, Steininger, F.F., Shcherba, I.G. and Kovac, M. 2004. Lithological Paleogeographic maps of Paratethys. 10 Maps Late Eocene to Pliocene, Volume 250. Courier Forschungsinstitut Senckenberg.

Popov, S.V., Sychevskaya, E.K., Akhmet'ev, M.A., Zaporozhets, N.I. and Golovina, L.A., 2008. Stratigraphy of the Maikop Group and Pteropoda Beds in Northern Azerbaijan. *Stratigraphy and Geological Correlation*, **16**, 664–677.

Popov, S.V., Rostovtseva, Y.V., Pinchuk, T.N. and Patina, I.S., 2019. Oligocene to Neogene paleogeography and depositional environments of the Euxinian part of Paratethys in Crimean – Caucasian junction. *Marine and Petroleum Geology*, **103**, 163-175.

Radke, M., Schaefer, R.G., Leythaeuser, D. and Teichmüller, M., 1980, Composition of soluble organic matter in coals: relation to rank and liptinite fluorescence. *Geochimica et Cosmochimica Acta*, **44**, 1787-1800.

Rampen, S.W., Schouten, S., Panoto, F.E., Muyzer, G., Campbell, C.N., Fehling, J. and Sinninghe Damsté, J.S., 2007. On the origin of 24-norcholestanes and their use as age-diagnostic biomarkers. *Geology*, **35**, 419-422.

Rampen, S.W., Abbas, B.A., Schouten, S. and Sinninghe Damsté, J.S., 2010. A comprehensive study of sterols in marine diatoms (Bacillariophyta): Implications for their use as tracers for diatom productivity. *Limnology and Oceanography*, **55**, 91-105.

Robinson, N., Eglinton, G., Brassell, S. and Cranwell, P.A., 1984. Dinoflagellate origin for sedimentary 4α-methylsteroids and 5α(H)-stanols. *Nature*, **308**, 419-422.

Sachsenhofer R.F., Popov S.V., Akhmetiev, M.A., Bechtel A., Gratzer, R., Gross, D., Horsfieldf, B., Rachetti, A., Rupprecht, B.J., Schaffar, W.B.H. and Zaporozhets, N.I., 2017. The type section of the Maikop Group (Oligocene-Lower Miocene) at the Belaya River (North Caucasus): Depositional environment and hydrocarbon potential. *AAPG Bulletin*, **101**, 289-319.

Sachsenhofer, R.F., Popov, S.V., Bechtel, A., Coric, S., Francu, J., Gratzer, R., Grunert, P., Kotarba, M., Mayer J., Pupp M. Rupprecht B.J. and Vincent, S.J. 2018a. Oligocene and Lower Miocene source rocks in the Paratethys: Palaeogeographic and stratigraphic controls. In: Simmons, M., (Ed.), Petroleum Geology of the Black Sea. *Geological Society London Special Publication*, **464**, 267-306. doi: 10.1144/SP464.1.

Sachsenhofer R.F., Popov S.V., Coric, S., Mayer, J., Misch, D., Morton, M.T., Pupp, M., Rauball, J. and Tari, G., 2018b. Paratethyan petroleum source rocks: An overview. *Journal Petroleum Geology*, **41**, 219-245. doi: 10.1111/jpg.12702.

Sachsenhofer, R.F., Bechtel, A., Gratzer, R., Enukidze, O., Janiashvili, A., Nachtmann, W., Sanishvili, A., Tevzadze, N. and Yukler, M.A., 2021. Petroleum systems in the Rioni and Kura basins of Georgia. *Journal of Petroleum Geology*, **44**, 3, 287-316, *this issue.*

Saint-Germès, M., 1998. Ètude sédimentologique et géochimique de la matière organique du bassin Maykopien (Oligocène-Miocène Inférieur) de la Crimée a l'Azerbaidjan. Mémoires des Sciences de la Terre. Académie de Paris Université Pierre et Marie Curie. 295 pp.

Saint-Germès, M., Baudin, F., Bazhenova, O., Derenne, S., Fadeeva, N. and Largeau, C., 2002. Origine et processus de préservation de la matière organique amorphe dans la Série de Maykop (Oligocène-Miocène inférieur) du Précaucase et de l'Azerbaïdjan. *Bull. Soc. géol. France* **173**, 423-436.

Schouten, S., van der Maarel, M.J, Huber, R. and Sinninghe Damsté, J.S, 1997. 2,6,10,15,19-pentamethylicosenes in Methanolobus bombayensis, a marine methanogenic archaeon, and in Methanosarcina mazei. *Organic Geochemistry*, **26**, 409-414.

Selby, D. and Creaser, R.A., 2003. Re-Os geochronology of organic rich sediments: an evaluation of organic matter analysis methods. *Chemical Geology*, **200**, 225-240.

Selly, R.C. and Sonnenberg, S.A., 2015. Elements of Petroleum Geology, 3rd Ed. Academic Press, 526 pp. ISBN: 9780123860316.

Shcherbinina, E., Gavrilov, Y., Iakovleva, A. and Pokrovsky, B., 2016. Environmental dynamics during the Paleocene–Eocene thermal maximum (PETM) in the northeastern Peri-Tethys revealed by high-resolution micropalaeontological and geochemical studies of a Caucasian key section. *Palaeogeography, Palaeoclimatology, Palaeoecology*, **456**, 60-81.

Shcherbinina, E., Iakovleva, A., Gavrilov, Y., Golovanova, O., and Muzylöv, N., 2020. Lower Eocene sedimentary succession and microfossil biostratigraphy in the central northern Caucasus basin. *Geologica Acta*, **18.1**, 1-15, DOI: 10.1344/GeologicaActa2020.18.1

Sinninghe Damsté, J.S., Kock-Van Dalen, A.C., de Leeuw, J.W., Schenk, P.A., Guoying, S., Brassell, S.C., 1987. The identification of mono-, di-, and trimethyl 2-methyl-2-(4,8,12-trimethyltridecyl)chromans and their occurrence in geosphere. *Geochimica et Cosmochimica Acta*, **51**, 2393–2400.

Smith-Rouch, L.S., 2006, Oligocene–Miocene Maykop/Diatom Total Petroleum System of the South Caspian Basin Province, Azerbaijan, Iran, and Turkmenistan. *U.S. Geological Survey Bulletin* 2201-I, 27 p.

Smoliar, M.I., Walker, R.J. and Morgan, J.W., 1996. Re-Os ages of group IIA, IIIA, IVA, and IVB iron meteorites. *Science*, **271**, 1099–1102.

Stein, R., 1990. Organic carbon content/sedimentation rate relationship and its paleoenvironmental significance for marine sediments. *Geo-Marine Letters*, **10**, 37-44.

Taylor, G.H., Teichmüller, M., Davis, A., Diessel, C.F.K., Littke, R. and Robert, P., 1998. Organic Petrology. Gebrüder Borntraeger, Berlin, 704 pp.

Thiel, V., Peckmann, J., Seifert, R., Wehrung, P., Reitner, J. and Michaelis, W., 1999. Highly isotopically depleted isoprenoids: Molecular markers for ancient methane venting. *Geochimica et Cosmochimica Acta*, **63**, 3959-3966.

VAN BAAK, C.G.C., STOICA, M., GROTHE, A., ALIYEVA, E. AND KRIJGSMAN, W., 2016. Mediterranean-Paratethys connectivity during the Messinian salinity crisis: The Pontian of Azerbaijan. *Global and Planetary Change*, **141**, 63-81.

VAN BAAK, C.G.C., KRIJGSMAN, W., MAGYAR, I., SZTANÓ, O., GOLOVINA, L.A., GROTHE, A., HOYLE, T.M., MANDIC, O., PATINA, I.S., POPOV, S.V., RADIONOVA, E.P., STOICA, M. AND VASILIEV, I., 2017. Paratethys response to the Messinian salinity crisis. *Earth-Science Reviews*, **172**, 193-223.

VERMEESCH, P., 2018. IsoplotR: A free and open toolbox for geochronology. *Geoscience Frontiers*, **9**, 1479-1493.

VINCENT, S.J. AND KAYE, M.N.D., 2017. Source rock evaluation of Late Middle Eocene to Early Miocene mudstones from the northeastern margin of the Eastern Black Sea. In: Simmons, M. et al. (Eds.), *Geol. Soc. Lond. Spec. Publ.*, **464**, 329-363. https://doi.org/10.1144/SP464.7

VÖLKENING, J., WALCZYK, T. AND HEUMANN, K.G., 1991. Osmium isotope ratio determinations by negative thermal ionization mass spectrometry. *International Journal of Mass Spectrometry and Ion Processes,* **105**, 147-159.

VOLKMAN, J.K. AND MAXWELL, J.R., 1986. Acyclic isoprenoids as biological markers. In: R. B. Johns (Ed.), Biological Markers in the Sedimentary Record , Elsevier, New York, pp. 1-42.

VOLKMAN, J.K, BARNETT, S.M. AND DUNSTAN, G.A., 1994. C_{25} and C_{30} highly branched isoprenoid alkenes in laboratory cultures of two marine diatoms. *Organic Geochemistry,* **21**, 407-413.

WASHBURN, A.M., HUDSON, S.M., SELBY, D., ABDULLAYEV, N. AND SHIYANOVA, N., 2018. Re-Os geochronology and chemostratigraphy of the Maikop Series source rocks of eastern Azerbaijan [Extended Abstract]. *Journal of Petroleum Geology*, **41** (3), 411-416.

WASHBURN, A.M., HUDSON, S.M., SELBY, D., ABDULLAYEV, N. AND SHIYANOVA, N., 2019. Constraining the timing and depositional conditions of the Maikop formation within the Kura Basin, eastern Azerbaijan, through the application of Re-Os geochronology and chemostratigraphy. *Journal of Petroleum Geology*, **42**(3), 281-300.

WAVREK, D.A., CURTISS, D.K., GULIYEV, I.S. AND FEYZULLAYEV, A.A., 1998. Maikop/Diatom-Productive Series (!) Petroleum System, South Caspian Basin, Azerbaijan. *AAPG Bulletin,* **82**, 2.

WEBER, V.V., 1935. Geological Map of the Kabristan. *Tr. NGRI. Series A*, **62**, 1-300.

WEBER, V.V, 1941. The Miocene of Kabristan and the Apsheron Peninsula (in Russian). In: Rengarten, V.P. (Ed.), Geology of the USSR, Vol. 10, Caucasus. Moscow - Leningrad, pp. 267-273.

ZAPOROZHETS, N.I. AND AKHMETIEV, M.A., 2015. Assemblages of organic-walled phytoplankton, pollen, and spores from the Solenovian Horizon (Lower Oligocene) of Western Eurasia. *Stratigraphy and Geological Correlation*, **23**, 326-250, doi:10.1134/S0869593815030077.

ZOLITSCHKA, B., 1998. Paläoklimatische Bedeutung laminierter Sedimente. Holzmaar (Eifel, Deutschland), Lake C2 (Nordwest-Territorien, Kanada) und Lago Grande di Monticchio (Basilicata, Italien). Bornträger, Berlin, 176 pp.